Vol.2, No.3, March-2024

APPLIED SCIENCES RESEARCH PERIODICALS

TABLE OF CONTENTS

EDITORIAL BOARD

DISCLAIMER

All the manuscripts are published in good faith and intentions to promote and encourage research around the globe. The contributions are property of their respective authors/owners and Applied Sciences Research Periodicals (ASRP) is not responsible for any content that hurts someone's views or feelings. Authors are responsible for if any plagiarism is found in published material.

Applied Sciences Research Periodicals – ISSN 3033-330X
March 2024, Vol. 2, No. 3, pp. 01-07

Protective Effect of Zingiber Officinale Extract on Streptozotocin Induced Diabetes Mellitus in Mice

Samia Elzwi[1] and Amina Elzwi[2]

1. Department of Pharmacology, University of Benghazi, Libya
2. Faculty of Pharmacy, University of Benghazi, Libya

Abstract:
Spices, the predominant flavoring, coloring, and aromatic agents in food and beverages are now gaining importance for their diversified uses. Ginger (Zingiber Officinale) is a medicinal plant that has been widely used in Chinese, and Tibb Unani herbal medicines all over the world, since antiquity, for a wide array of unrelated ailments that include muscular aches, sore throat, constipation, arthritis, indigestion, vomiting and infectious diseases. Currently, there is a renewed interest in ginger, and several scientific investigations aimed at isolation and identification of active constituents of ginger, scientific verification of its pharmacological actions and of its constituents, and verification of the basis of the use of ginger in several diseases and conditions most common is use of ginger as complementary therapy in diabetes patients is now increasing due to less side effect comparing with antidiabetic drugs. Streptozotocin enter the B cell via glucose transporter (GLUT2) and cause alkylation of DNA. DNA damage induced by activation of poly ADP-ribosylation; a process is more important for diabetogenicity of streptpzotocin than DNA damage itself.

INTRODUCTION

Ginger grows best in tropical and subtropical areas, which have good rainfall with hot and humid conditions during the summer season. It is a member of Zingiberaceae family originated in Southeast Asia and has been introduced to many parts of the globe where it proliferates in suitable environment. Belief in the medicinal properties of ginger existed in ancient Indian and oriental cultures where ginger has been used alone or as a component in herbal remedies [1].

This practice continues today in many areas of the world including Africa, Brazil, China and, Mexico. Ginger has introduced to Europe and other areas by Dutch, Portuguese Arab and Spanish explorers or traders from around the 13th to 16th centuries [2]. Carbohydrates Starch is the major constituent up to 50%. Oleoresin Gingerol homologues (major, about 33%) include derivatives with methyl side chain, shogaol homologues (dehydration products of gingerols), zingerone (degradation product of gingerols) ,1- dehydrogingerdione and 6- ginger sulfonic acid. Lipids 6-8% They include free fatty acids e.g. palmitic acid, oleic acid, linoleic acid, caprylic acid, capric acid, lauric acid, myristic acid, pentadecanoic acid, heptadecanoic acid, stearic acid, linolenic acid, arachidonic acid, triglycerides, phosphatidic acid, lecithin and ginger glycolipids A, B and C. Ulcer are caused due to imbalance between aggressive factors (hydrochloric acid, pepsin, gastrin, steroidal anti-inflammatory drugs, and ethanol) and defensive factor of gastric mucosa (prostaglandin, mucus, bicarbonate) [3].

Figure (1): Zingiber officinale leaves

There are several herbal ayuvedic preparation which have a protective effect against gastric mucosal injury [4]. Herbal medicine is now used by up to 50% of the Western population in a number of instances 10% for treatment or prevention of digestive disorders [5]. Today, pharmacopoeias of a number of different countries list ginger extract for various digestive disease [6]. Aromatic, spasmolytic and carminative properties of ginger are probably responsible for the therapeutic application in digestive tract ailments [.7,8].

Figure (2): Fresh ginger rhizome

Streptozotocin (STZ) was initially isolated from Streptomyces achromogenes in 1960, with its diabetogenic properties not described until 1963 [9] This action was characterized by Junod, [10.11]. showing that the diabetogenic effects are due to selective destruction of pancreatic islet β-cells. As a result of this action, the animals experience insulin deficiency, hyperglycemia, polydipsia, and polyuria, all of which are characteristic of human type 1 diabetes mellitus [12]

Streptozotocin enter the B cell via a glucose transporter (GLUCT2) and cause alkylation of DNA. DNA damage induced activation of poly ADP- ribosylation, a process that is important for diabetogenicity of streptzotocin than DNA damage itself

Poly ADP ribosylation leads to depletion of cellular NAD+ and ATP.

Enhanced ATP dephosphorylation after streptozotocin treatment supplies substrate for xanthine oxidase resulting in formation of superoxide radicals, consequently hydrogen peroxide and hydroxyl radicals are also generated.

Streptzotocin liberates toxic amount of nitric oxide that inhibits aconitase activity and participates in DNA damage

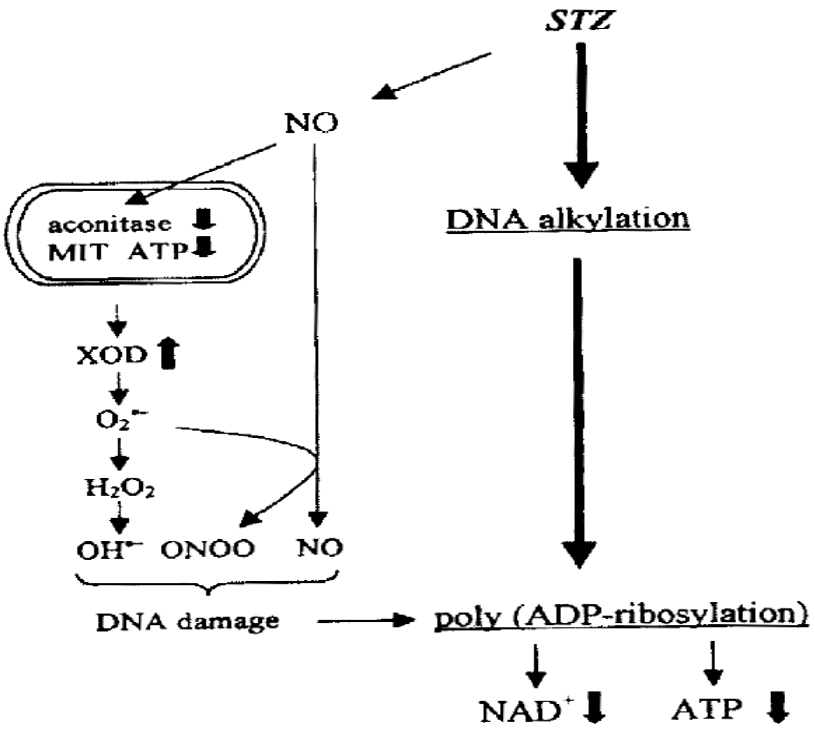

Figure (3): Mechanism of action of streptozoticin

MATERIAL AND METHOD

Experimental an Albino mouse of either sex weighing 20-30 g, and male Wistar strain rats Weighing 200-250 g were maintained in the animal house of Faculty of Medicine – Al Arab Medical University, Benghazi, Libya. The mice and Rats were bred in the faculty animal house. All animals were housed in Standard polypropylene cages (48×35×22 cm) and kept under controlled Room temperature (20±5 ◦C; relative humidity 60-70%) in a 12 h light-dark Cycle. The animals were given a standard laboratory diet and free water Food was withdrawn 12 h before and during the experimental hours. e Maceration method: In this method fresh ginger rhizome was cut into small pieces, dried, and then pulverized into coarse powder and weighing about 400 g of powder. It was macerated in 1000 ml hydroalcoholic solution (70% Ethanol, 30% distilled water) for seventy-two hours. The extract was then shaked, filtered by using filter paper and the solution was evaporated in a rotatory evaporator under reduced pressure until dryness. Evaporation and removal of the solvent give hydroalcoholic extract of ginger out of 400 g of crude plant, 8 g of hydroalcoholic extract of ginger were obtained and kept for use in pharmacological experiments (Iranian Herbal Pharmacopea).

The mice were divided into five groups each contain six mice

1. Control group: given normal saline is a dose of 0.1 ml each mouse
2. The streptozotocin in a dose of 180mg/ kg was used with sodium citrate pH 4.5, 0.1 ml is given intraperitoneal to each mouse
3. Extract of ginger given in a dose of 300mg/kg (orally p.o) and then after three hours blood glucose was assessed.
4. Extract of ginger given in a dose of 300mg/kg (intraperitonealy i.p) and then after three hours blood glucose was assessed.
5. Glibecclamide was given in a dose of 0.5mg/kg by dissolving 5mg of glibenclamide tablets in 50ml of distilled water and each mouse given 0.3 ml orally. Then after three hours, blood glucose was assessed.

STATISTICAL ANALYSIS

The experimental results were expressed as the mean± S.E.M and are accompanied by the number of observations. Data were assessed by the method of one-way analysis of variance (ANOVA), if this analysis indicated significant difference among the group means, then each group was compared by rather LSD or paried sample test. A.P value less than 0.05 was considered statistically significant. P value less than 0.001 was considered statistically highly significant.

As shown in the figure (4) highly significant ($p<0.001$) increase in the blood glucose level in the streptozotocin treated compared with control group.

The data also reveals significant reduction in the blood glucose level in the ginger treated (p.o) c ($p<0.05$) compared with streptozotocin treated group.

The data also shows highly significant ($p<0.001$) reduction in the blood glucose level in glibenclamide treated group compared with streptozotocin treated group

Figure (4): Effect of oral administration of ginger extract on streptozotocin-induced diabetes mellitus in mice

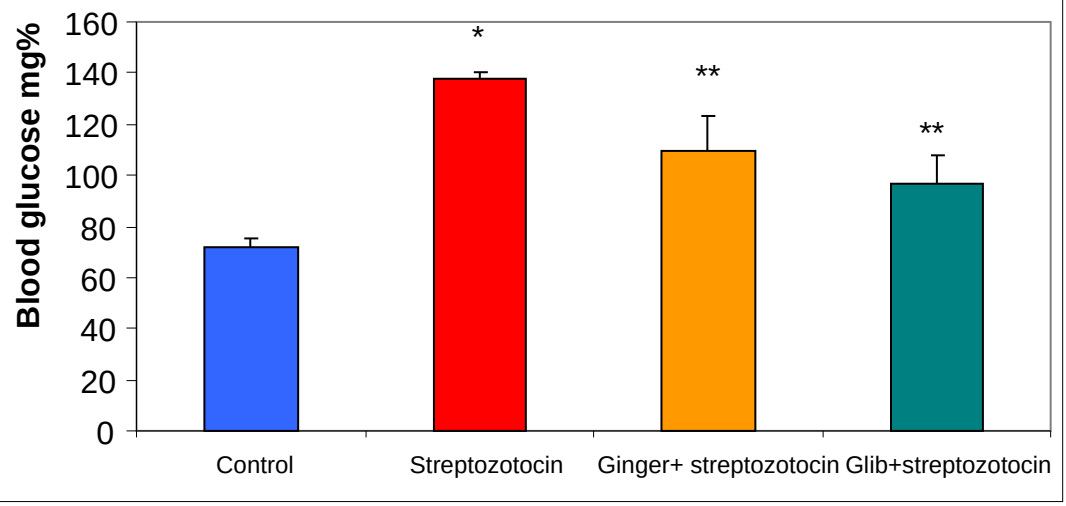

Results in the figure (5) shows highly significant increase($p<0.001$) in the blood glucose level in the streptozotocin compared with control

The data also reveals non-significant reduction ($p>0.05$) in the blood glucose level in ginger treated (i.p) compared with streptozotocin treated group.

The data shows nonsignificant difference ($p>0.05$) between ginger extract (p.o and i.p) and glibenclamide.

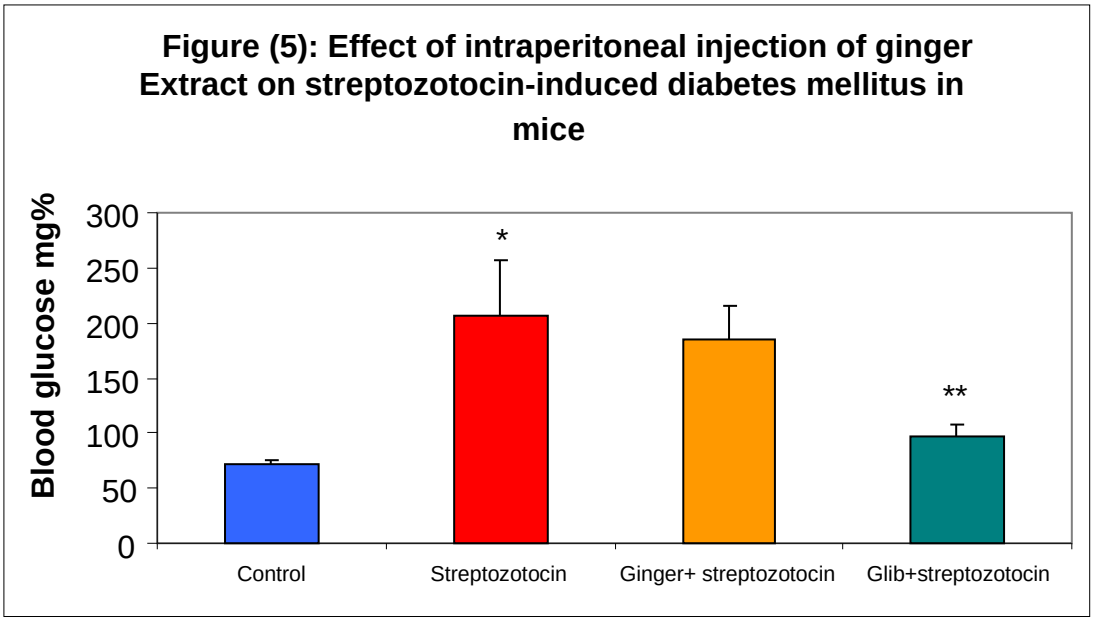

DISCUSSION

In this model of diabetes induction, we use streptozotocin as its commonly used agent and ginger extract showed significant reduction in blood glucose. Our results in accordance with study of hypoglycemic effect of ginger in streptozotocin – induced persistent hyperglycemia in rats by Al-Amin [13]. ginger in a dose of 500mg/kg was significant effective in lowering serum glucose. The ginger treatment also resulted in significant reduction in urine protein levels and decreased both water intake and urine output in the streptozotocin – induced diabetic rats. In addition, raw ginger was effective in reversing the diabetic proteinuria observed in the diabetic rats. Thus, ginger may be of value in managing the effects of diabetic complications in human subjects.

The hypoglycemic effect of plant extract was investigated in rats by using streptozotocin as models of persistent hyperglycemia, ginger extract at a dose of 50- 800 mg/kg caused dose related significant hypoglycemia in normal and diabetic rats. The finding of this animal study indicated that zingiber officinale rhizome extract possess hypoglycemic properties and thus lend pharmacological support to folkoric, ethnomedical uses of ginger in the management and control of type 2 diabetes mellius [14]

Additionally, another study assessed the antihyperglycemic activity of its aqueous Extract given orally (daily) to streptozotocin (STZ)- induced diabetic rats at three different doses (100, 300, and 500 mg/kg body weight) For a duration of 30 days. After the rats were given 500 mg/kg, a dose dependent antihyperglycaemic effect showed a drop in plasma glucose levels by 38 and 68% on the 15th and 30th day, respectively.

ZO dramatically boosted ($P < 0•05$) the activities of phosphofructokinase, pyruvate kinase, and glucokinase in STZ- diabetic rats, whereas the activities of these enzymes dropped in diabetic controls by 94, 53, and 61%, respectively, as compared to normal controls.

Thus, by influencing the activities of glycolytic enzymes, the current study demonstrated that gi nger is a viable phytomedicine for the treatment of diabetes. [15].

Furthermore, the aqueous extract of raw ginger was administered daily (500 mg/kg, intraperitoneally) for a period of 7 weeks to streptozotocin (STZ)-induced diabetic rats. Fasting blood serum was analyzed for blood glucose, cholesterol and triacylglycerol levels. The STZ-injected rats exhibited hyperglycemia accompanied with weight loss, indicating their diabetic condition. At a dose of 500 mg/kg, raw ginger was significantly effective in lowering serum glucose, cholesterol and triacylglycerol levels in the ginger-treated diabetic rats compared with the control diabetic rats. The ginger treatment also resulted in a significant reduction in urine protein levels. In addition, the ginger-treated diabetic rats sustained their initial weights during the treatment period. Moreover, ginger decreased both water intake and urine output in the STZ-induced diabetic rats [16].

6-Shogaol exhibited an antidiabetic effect by significantly decreased the level of blood glucose, body weight and attenuated pathological changes to the normal levels in the diabetic mice, and has effect against pancreas, kidney, liver damage in the diabetic mice. Since, 6-shogaol prevented the damage for STZ induced stress [17].

REFERENCES

1- Ali, B, H, G. Blunden, M. O. Tanira and A. Nemmar Some phytochemical, pharmacological and toxicological properities of ginger (2007) (Zingiber officinale); vol (2) 333-340

2- Suekawa, M. Pharmacological action of pungent constituents (6) – Gingerol and (6) Shogaol. Journal of phramacobiodynamic 1984, 7 (11), 836-848f recent research. Food Chem Toxicol; 18: 17950516.0

3- Dennis, V. C, Awang. Introduction to herbs part two (2007). Walgreen Health Initiative; 7:60-66

4- Yan Liu, Jincheng Liu, and Yongqing Zhang (2019). Research Progress on Chemical Constituents of Zingiber officinale Roscoe (2019). BioMed Research International, Article ID 5370823, 21.

5- Connell D. The chemistry of essential oil and oleoresin of ginger (Zingiber officinale Roscoe (1970) . Flavor Industry; 1:677-93

6- Iranian Herbal Pharmacopea Scientific Committee' Iranian Herbal Pharmacopea'. 1st ed. Iranian Ministry of health Publication; 2002:25

7. Shetty R,Kumar KV, Naidu MUR and Ratnakar KS.Effect of Gingko Bilbo extract on ethanol – induced gastric lesions in rats (2000), Indian j pharmacol ;32:313-7.

8. Langmead and Rampton DS. Herbal treatment in gastrointestinal and liver diseases- benefit and dangers (2001). Aliment Pharmacol Ther: 15:1239-1252.

9. RAKIETEN N, RAKIETEN ML, NADKARNI MR. Studies on the diabetogenic action of streptozotocin (1963). Cancer Chemother Rep. 1963 May; 29:91-8.

10. Junod, A., Lambert, A. E., Stauffacher, W., & Renold, A. E. (1969). Diabetogenic action of streptozotocin: Relationship of dose to metabolic response. Journal of ClinicaInvestigation, 48, 2129–2139. doi: 10.1172/ JCI106180.

11. Junod, A., Lambert, A. E., Orci, L., Pictet, R., Gonet, A. E., & Renold, A. E. (1967). Studies of the diabetogenic action of streptozotocin. Proceedings of the Society for Experimental Biology and Medicine, 126, 201–205. doi: 10.3181/ 00379727-126-32401l.

12. Kolb, H. (1987). Mouse models of insulin dependent diabetes: Low-dose streptozocin-induced diabetes and nonobese diabetic (NOD) mice. Diabetes Metabolism Reviews, 3, 751–778. doi: 10.1002/dmr.5610030308.

13. Al-Amin, ZM,Thomson, M, Al-Qattan, K.K.Peltonen-Shalalby.R andAli , M. Anti-diabetic and hypolipidemic properities of ginger (Zingiber officinale) in streptpzotocin- induced diabetes rats. British journal of nutrition;96(4) 660-666.

14. John Aand O.Ojewole . Analgesic, anti-inflammatory and hypoglycemic effects of ethanol extract of zingiber officinale rhizome in mice and rats (2006). Wiley InterScience ;20(9): 764-72.

15. Nafiu Bidemi Abdulrazaq, Maung Maung Cho, Ni Ni Win, Rahela Zaman andMohammad Tariqur Rahman Beneficial effects of ginger (Zingiber officinale) on carbohydrate metabolism in streptozotocin-induced diabetic rats (2011). British journal of Nutrition volume 108 issue 7.

16. Zainab M. Al-Amin, Martha Thomson, Khaled K. Al-Qattan, Riitta Peltonen-Shalaby and Muslim Ali. Anti-diabetic and hypolipidaemic properties of ginger (Zingiber officinale) in streptozotocin-induced diabetic rats (2007). British journal of Nutrition volume96 issue4 Published online by Cambridge University Press: 08 March 2007.

17. Jun-Koo Yi, Zae-Young Ryoo, Jae-Jung Ha, Dong-Yep Oh Myoung-Ok Kim &Sung-Hyun Kim. Beneficial effects of 6-shogaol on hyperglycemia, islet morphology and apoptosis in some tissues of streptozotocin-induced diabetic mice (2019) Diabetology & Metabolic Syndrome volume 11, Article number: 15 (2019)

Applied Sciences Research Periodicals – ISSN 3033-330X
March 2024, Vol. 2, No. 3, pp. 08-21

Malaria Surveillance System Evaluation in Ankober Woreda North Shewa, Amhara Region, Ethiopia, 2022

Tesfahun Abye, Bezawit Hailegiorgis, Bereket Taye, & Tigist Abera

Abstract:
Background: Malaria is a major public health concern worldwide, with the African region accounting for the majority of cases. Routine malaria surveillance data is crucial for assessing incidence and trends over time and detecting cases early for prompt management. The purpose of evaluating malaria surveillance systems is to assess how well they operate to meet their objectives and ensure efficient and effective monitoring of problems. This study aimed to evaluate and assess the performance of the existing malaria surveillance system and the status of surveillance attributes of malaria in Ankober woreda, North Shewa, Amhara. General objective: To evaluate and assess the performance of the existing Malaria surveillance system and the status of surveillance attributes of malaria in Ankober woreda, North Shewa, Amhara from December 16-26 2022. Method: A descriptive cross-sectional study were conducted from December 16-26, 2022. Ankober woreda were selected randomly among 239 malaria elimination targeted districts and total of nine health facilities were selected. The data were collected from surveillance officers in the selected health facilities using CDC surveillance system evaluation guideline check-list. Result: The results showed that case definitions were posted in all health centers, and understanding of them was good. The woreda reported a total of 26 confirmed malaria cases among 195 clinically suspected cases and zero deaths in 2014 EFY. The overall completeness and timeliness of the woreda surveillance for 2022 were 100% and 97%, respectively. Malaria epidemic monitoring charts were used to detect changes in cases but not analyzed by place and person. Irregular feedback and supportive supervision were conducted. High staff turnover and less trained and poorly incentivized health personnel with poor motivation and job satisfaction were found. The surveillance system was found to be useful, simple, flexible, acceptable, sensitive, and representative to all surveillance officers. Conclusion: Malaria surveillance system found to be satisfactory to achieve the intended objective of surveillance for public health action. Most surveillance system attributes are good. Working surveillance as an additional job and reduced training opportunity added with poor incentive mechanism will make low motivation and satisfaction with their job that definitely affect the stability of the system. The Malaria surveillance system presented in all assessed health institutions of Ankober woreda was found to be able to determine the magnitude of the disease for planning and intervention and detect change in malaria mortality and morbidity.

BACKGROUND

Public health surveillance is the ongoing, systematic collection, analysis, interpretation, and dissemination of data regarding a health-related event for use in public health action to reduce morbidity and mortality and to improve health(1). Public health surveillance systems have been developed to address a range of public health needs and is considered to be an essential public health function. The number and variety of Public health surveillance systems will likely increase with advances in electronic data interchange(2).

The objectives of having public health surveillance in a country are firstly to detect any disease outbreaks or unusual events and early warning of potential threats to public health which may be disease specific or multi-disease in nature, secondly to provide information which may be used to monitor and evaluate the impact of disease prevention and control program and thirdly to monitor trend in communicable disease over time to assess the present situation so that we can be effective in investigating, controlling, and preventing disease in the population and to link with public health action and to monitor progress towards disease control objectives(3).

Even though efforts to establish Malaria surveillance system was initiated in Ethiopia 1947 when the government issued quarantine rules, these efforts were not supported with appropriate resources thus; surveillance was limited in scope and usefulness. Lack of functional surveillance system that can guide timely and effective health intervention has been a common problem to the African region. Thus, the African States through the WHO Africa regional office (WHO/AFRO) made a resolution (resolution AFRO/RC48/R2) in September 1998 to develop an integrated disease surveillance and response (IDSR) initiative as a regional strategy to effectively control priority communicable diseases in the African region. The reason for Malaria inclusion under surveillance is due to its significant public health importance it poses and effective prevention and control measures it have(4).

Ethiopia had adapted a comprehensive strategy recommended by WHO for member state during the 48th assembly in 1998 for improving communicable diseases surveillance and response through Integrated Disease Surveillance and response (IDSR). After the implementation of IDSR, The Government of Federal Democratic Republic of Ethiopia has embarked country wide reform initiative using the Business Process Reengineering (BPR) as a tool in 2005(5).

Accordingly, federal ministry of health (FMoH) evaluates IDSR and recommend to establish Public Health Emergency Management (PHEM) as of 2009. One of the major activities of PHEM is to take over the disease's surveillance parallel to preparedness, response and rehabilitation in any health-related emergencies and outbreaks. Malaria was one of the diseases selected to be under surveillance system due to its huge burden (morbidity and mortality) The PHEM cascades down to regional level through regional health bureaus, with their zonal health departments and district health offices as shown in the diagram(6).

Malaria remains one of the most important causes of human morbidity and mortality with enormous medical, economic and emotional impact in the world. The World malaria report 2018 estimates that there were 219 million cases of malaria in 2017 globally(7). The WHO African Region accounted for most global cases of malaria (200 million or 92%), followed by the WHO South-East Asia Region with 5% of the cases. Malaria is the 2nd leading cause of death from infectious diseases in Africa, after HIV/AIDs. It continues to claim the lives of more than 435, 000 people each year, largely in Africa. The WHO African Region accounted for 93% of all malaria deaths in 2017. Although countries across the African Region have led a massive effort to expand access to malaria control, the findings of 2017 World Malaria report revealed an increase of 3.5 million cases of malaria in the ten highest burden African countries, as compared to 2016. Despite this increment, there are signs of progress as overall trends show that between 2010 and 2017, the estimated number of new cases of malaria in the African Region cases dropped from 206 million in 2010 to 200 million in 2017, and the number of malaria-related deaths fell from 555,000 to 403,000. Two countries in the Region (Ethiopia and Rwanda) are among 20 countries globally

that experienced a significant decrease in malaria cases (by more than 20%) and deaths in 2017 compared to 2016 (7).

In 2017, an estimated US$ 3.1 billion was invested in malaria control and elimination efforts globally by governments of malaria endemic countries and international partners. The level of investment in 2017 is far from what is required to reach the first two milestones of the Global technical strategy for malaria 2016–2030 (GTS); that is, a reduction of at least 40% in malaria case incidence and mortality rates globally by 2020, compared with 2015 levels(7). Empowering individuals and communities and engaging them to adopt and deploy simple and cost-effective interventions is key in filling existing implementation gaps. We need to accelerate progress as there are significant gaps in the implementation of measures to prevent malaria, and stagnating international and domestic funding for malaria prevention and control. Therefore, renewed political commitment to mobilize all necessary internal and external resources to eliminate malaria and increased investments on malaria prevention and control and ensure inter-sectoral and cross-border collaboration.

To respond to the challenge of rising cases in high-burden countries and reverse these trends, a 'high burden to high impact' (HBHI) country-led approach was launched in November 2018 Supported by WHO and the Roll Back Malaria Partnership, the response seeks to galvanize political will nationally and globally to reduce malaria deaths; it will also use strategic information to drive impact and implement the best global guidance, policies and strategies for malaria-endemic countries, as well as coordinated country responses.

Countries in the Region are continuing to carry out malaria testing and treatment and also relying on preventive measures such the distribution and use of insecticide-treated nets and indoor spraying with insecticides as key strategies in combatting malaria. Even though a considerable proportion of people at risk of malaria infection are not being protected, half of the people at risk of malaria across sub-Saharan Africa are now sleeping under insecticide-treated nets in 2017, as compared to 30% in 2010, indicating some success in behavior change and outreach campaigns. This progress needs to be sustained(8).

RATIONALE OF STUDY

The primary purpose of collecting data on malaria surveillance is for decision-making and action at the local level and evaluation of the system ensure that problems of malaria surveillance are being monitored efficiently and effectively(1). The information generated from malaria surveillance informs international financiers of malaria program and are an important determinant of future funding, regularly assess whether plans are progressing as expected or whether adjustments are required, allocate resources to the populations most in need in order to achieve the greatest possible public health impact, evaluate whether the surveillance objectives have been met and to learn what has worked and what has not, so that more efficient, effective program can be designed, advocate for investment in malaria surveillance and track progress toward elimination.(9) Malaria surveillance should be evaluated periodically, and the evaluation should include recommendations for improving quality, efficiency, and usefulness(10). Evaluation of Malaria surveillance system promotes the best use of data collection resources and focuses on how well the system operates to meet its purpose and objectives. Surveillance system evaluation allows us to define whether a specific system is useful for a particular public health initiative and is achieving the overarching goals of the public health program and the data collection objectives.

Routine malaria surveillance data is useful for assessing incidence and trends over time and stratification for targeting of malaria control(1).

One of the key GTS milestones for 2020 is elimination of malaria in at least ten countries that were malaria endemic in 2015. Accelerating the elimination of malaria, and eventually interrupting its transmission, requires data and information from surveillance systems to inform decisions on the optimal deployment and impact of interventions(11). Effective surveillance of malaria cases and deaths, and of key entomological and efficacy indicators, is essential for identifying which areas or population groups are at risk of malaria or are vulnerable to reduced efficacy of interventions and also for targeting resources for maximum impact. In turn, this allows for effective programmatic planning, including response to epidemics and intensification of control and prevention measures when necessary. A strong surveillance system requires high levels of access to care and case detection, and complete reporting of health information by all sectors, whether public or private (12). Monitoring and evaluation for core antimalarial interventions in-terms of coverage, quality and target is key and will be monitored to inform actions to be taken(13). Therefore, this project will evaluate the performance of the existing Malaria surveillance system and assess the status of surveillance system attributes of malaria in Ankober woreda, North Shewa, Amhara. The data generated by the study can be used for immediate public health action, program planning and evaluation, and formulating research hypotheses.

Objective of Malaria Surveillance System Evaluation

General Objective:

- Descriptive study to assess the implementation status of the existing Malaria surveillance system and the status of surveillance system attributes of malaria and describe constraints and challenges faced in the process of implementing malaria surveillance in Ankober woreda, North Shewa, Amhara from June-August 2022.

Specific Objectives:

- To assess the implementation status of core surveillance activities such as case detection, reporting, analysis and response system in the woreda
- To evaluate the status of surveillance system attributes of malaria
- To describe constraints and challenges faced in the process of implementing malaria surveillance

METHOD

Study Area

Malaria surveillance system evaluation were carried out in Ankober woreda of North Shewa in Amhara region. Ankober is one of the 24 woredas in North Shewa and the former seat of the Shewan kings, which is located 172km in Northeast of Addis ababa, the capital of Ethiopia and 42km east of zonal capital Debre/birhane at the elevation of 2,465. Ankober had served as a tent capital for six Shewan kings until Emperor Minilik II moved to Entoto in 1878. Several churches rich in paintings and manuscripts, along with the splendid geographical feature are awesome assets of Ankober. From the top of Ankober Palace Lodge, you can clearly see the separation point of the highland part of Ethiopia from the rift valley gorge and there is a chance to see the Gelada baboon troops, the endemic primates to Ethiopia. The Woreda is constructed by 3 urban & 19 rural kebeles. The woreda has 6 health center, 19 health post, 6 private clinic, 1 pharmacy, 77- health professional and 34- health extension workers. The woreda has road facility and

electricity. Total population of the woreda is 92,132 and population who lives in Malarious area is 60,689 (65.87%).

Study Design and Period

A descriptive cross-sectional study was conducted from December 16-26, 2022 to evaluate the current status malaria surveillance system.

Source and Study Population

The source population for the study is the 239 malaria elimination targeted districts and the study population is Ankober woreda health office and selected health facilities (health centers and health posts) in the woreda.

Sample Size and Sampling Technique

Among the 239 malaria elimination targeted woredas, Ankober woreda were selected by simple random sampling. Then, a total of nine health facilities (three health center and six health posts) were selected presenting with good and poor surveillance practice as judged by regional and woreda health offices, which is 36% of the total government health facilities (25). The study subjects were the woreda health office and nine selected health facilities. In each study site, health professionals working as a PHEM officer were asked to respond to the questions.

Inclusion and Exclusion Criteria

Public Health Emergency Management Officers/ Surveillance officers irrespective of their profession will be asked the questions. Officers who are in annual leave, critically sick or on field mission were replaced by assistants and if assistant officers are not available, the health facility were replaced by another facility.

Data Collection Method and Analysis

The data were collected from surveillance officers in the selected health facilities and staffs of the health institutions (PHEM officers and HEWs) using CDC surveillance system evaluation guideline check-list. Secondary data sources such as surveillance report completeness and timeliness as well as malaria surveillance data, supervision report, written feedbacks, preparedness plans were also be reviewed. Collected data were transferred in to electronic version and descriptive analysis were performed using Microsoft excel 2013.

Ethical Clearance

Ethical clearance to conduct the study were obtained from Ethiopian Public Health Institute and again permission from zonal health departments were obtained. Request letter were provided for the selected health office and health facilities for their participation on the study.

Consent Form:

Detailed information about the study were provided to PHEM/surveillance officers' that the study has no risk to any of respondents and specific written consent were provided attached at the end of the document.

Conflict of Interest:

The principal investigator declared that, there is no conflict of interest for this project.

Funding Declaration:
This research was not funded by any external sources

Author Contribution Declaration:
T.A conceived and designed the study. B.H support the analysis and edited the manuscript. B.T, T.A has reviewed and approve the manuscript.

Case Definition
Standard Case Definition of Malaria:
Any person with fever or fever with headache, rigor, back pain, chills, sweats, myalgia, nausea, and vomiting diagnosed clinically as malaria.

Confirmed Cases of Malaria:
A suspected case confirmed by microscopy or RDT for plasmodium parasites.

Operational Definitions
Simplicity:
The simplicity of a public health surveillance system refers to both its structure and ease of operation surveillance system.

Acceptability:
Reflects the willingness of individuals and institutions to participate in the surveillance system.

Data quality:
Data quality is the completeness and validity of the data recorded in the public health surveillance system.

Representativeness:
Is the ability of the system to describe health events accurately in terms of time, place and person.

Sensitivity:
Sensitivity is the capacity of the system to detect the highest proportion of true cases.

Stability:
Refers to the reliability (i.e., the ability to collect, manage, and provide data properly without failure) and availability (the ability to be operational when it is needed) of the public health surveillance system.

Timeliness:
Is the ability of the system to trigger appropriate action in time.

Usefulness:
Refers to the relevance of the system in terms of feeding information for action.

Predictive Value Positive:
Is the proportion of reported cases that actually have the health-related event under surveillance.

Flexibility:
Is the ability of the system to adapt to changing needs such as the addition of a new disease, the collection of additional data, and change in case definition.

Completeness:
Proportion of all expected data reports that were submitted to public health surveillance.

Data Quality Control
Data collected at every level were crosschecked with the data available at national level and zonal level and completeness of the information after every interview were checked.

Dissemination of Findings
Once the final report is confirmed by the academic mentor, written report will be forwarded to North Shewa health department, Ankober woreda health offices, EPHI and Saint Paul's Hospital Millennium Medical College, department of public health.

Budget Summery
The project was costed a total of about $1,479.42 equivalent to 41,423.76 Ethiopian birr and had got a free technical support and mentoring from volunteer senior FETP graduates and colleagues.

RESULT

Availability of Surveillance Manuals, Forms and Registers
Malaria is reported on weekly bases however during epidemic the reporting will be changed to daily basis in Ankober woreda. Among the assessed 9 health facilities and woreda health office, only the woreda had national PHEM guideline but two health centers and a single health post had Amharic version of PHEM guideline prepared by APHI. However, the remaining 1 health center and 5 health posts didn't have the national PHEM guideline as well as regional Amharic version. All visited three health centers had standard malaria diagnosis and treatment guideline and only Gorebela health center had malaria epidemic prevention and control guideline. There was no shortage of weekly reporting formats in the past six months in 7 (77.78%) of nine visited health facilities and health office but all health facilities didn't have case investigation form, line list, and daily epidemic reporting format except the woreda health office. There were standardized registers to record the basic data elements of malaria at all the visited health centers but not in HPs.

Case Detection, Confirmation and Registration
The surveillance system capture data on cases of malaria suspected fever case, total malaria cases (confirmed and clinical) for outpatient, inpatient and deaths and confirmed malaria cases by species. Aliyu Amba Health center, Gorebela health center and woreda health office had Malaria case definitions posted and understanding of this case definition at those visited health facility was good as explained by some of health workers working in OPDs during the time of field visit. On the other hand, from all the assessed health posts only 3 (50%) of 6 had the community case definition for malaria but health extension workers didn't use the case definition for treatment of cases except detection and referring to the HCs. The health professionals were detecting any suspected cases of malaria using the case definition and laboratory investigation (BF and RDT) at the health center level but none of laboratory investigation is done at health post level. In all visited health posts, health extension workers complained of lack of RDT and obliged to refer most of malaria suspected cases to health center for microscopic (BF) or RDT investigation.

The surveillance system encourages community participation to detect and respond to disease epidemics through health extension program. All health centers properly register case records using standard registers however in health posts, they only use patient history cards as a register. Contacts of malaria cases are not investigated and contact screening were not done and there is no either paper based or electronic patient registry in all visited health posts. Entomological investigation not done yet.

Reporting and Quality of Data

The woreda did received a total of 468 weekly reports from six government health centers and three private clinics and had sent a total of 52 weekly reports to zonal health departments in the past one year (2022/2023). The woreda did received and report a total of 26 confirmed malaria cases (11 Pf and 15 PV) among 195 clinically suspected cases and zero deaths in 2014 EFY. The overall completeness and timeliness of the woreda for 2022 were 100% (21rep/21wk) and 97% respectively as reported from woreda health office. All health facilities report weekly malaria cases via SMS or phone call but the woreda reports malaria cases to zonal health department via E-mail or paper based integrated with other weekly reportable diseases but may use phone in some cases and for immediately reportable cases. Reporting time of malaria from health facility to Woreda health office were every Monday till mid-day and from woreda health office to zonal health department every Tuesday till mid-day and to the Regional Health Bureau every Wednesday till mid-day and finally to EPHI every Thursday till mid-day.

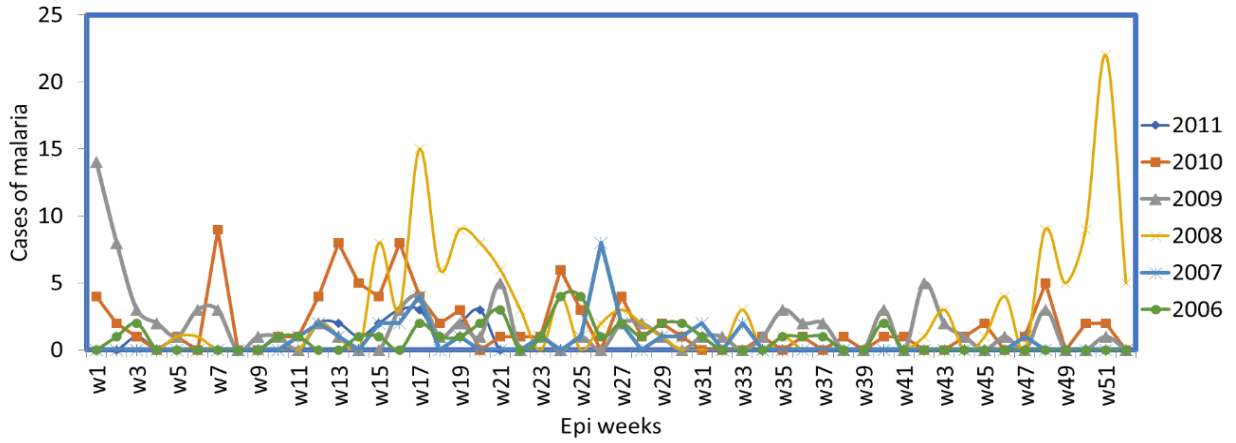

Figure 1: Trends of confirmed malaria cases by WHO epidemiological week from 20011-2014 EFY in Ankober woreda

Data quality at health facility level was assessed by completeness of reporting forms. All variables of the reported registers are properly and completely filled in Aliyu amba and Gorebela health centers but in Gorgo health center, the copy of reports was not found in the weekly reporting formats for 5 weeks. The information registered on the weekly reporting form matches with patient record at the health facility and data at zonal level confirmed by documented reports.

Data Analysis

In all visited health facilities, there was no a responsible person for data analysis but all health centers (not health posts) use malaria epidemic monitoring chart for cases trend monitoring and used to detect if there is an epidemic. In the woreda health office data analysis made on irregular basis by PHEM officer but analysis was not complete i.e., done only by time (not incorporating place and person). The information collected was utilized to monitor threshold which is done only

by doubling previous year same season cases but not using the third quartile of the five years morbidity data.

Epidemic Preparedness and Response:

The Woreda health office had a plan for epidemic preparedness and response supported by malaria emergency budget but all visited health centers and health posts has no epidemic preparedness andresponse plan. Even though the Woreda health office had budget for malaria emergence, in case of experiencing any emergency other than malaria, the Woreda mobilized the budget for response activity. Woreda health office have non-functional/deactivated rapid response team and all of the assessed health centers (not include health posts) have non-functional emergency/epidemic management committee but will be revitalized when emergency happened. There was no vehicle assigned for emergency response at Woreda health office. There was no malaria outbreak in the past 2022 but there was measles outbreak which is investigated and responded timely and confirmed for the presence of RRT and epidemic management committee (EMC) by meeting minute.

Feedback and Supervision

Both verbal and written feedback integrated with routine supportive supervision was given to all visited health facilities from woreda PHEM Core Process together with other departments on quarterly basis but evidence of sample reports found only in two assessed health centers. The zonal health department did give feedback to Ankober woreda on weekly basis with sufficient evidence of reports. The assessment did find a sample report of a recent supportive supervision in 7 (77.78%) of 9 health facilities but it was not specifically on malaria surveillance. Similarly, health center made supervision once a month to each respective health posts in the catchment area.

Training:

All assessed health facility focal persons, health care providers, and health extension workers who are assigned as a focal point for surveillance responded that none of them got a formal training other than having an orientation on surveillance and epidemic management and most surveillance focal persons participating in the study were new for the system and this is due to high staff turnover as recognized by participants. Mobile card expense for reporting and reduced training opportunity added with non-incentivized health personnel is difficult for operation. Woreda health office PHEM Core Process owner did get a training on different topics (malaria elimination, basic level PHEM training) but didn't have a training on frontline field epidemiology training program (FFETP).

Resources Used for Surveillance System

All visited health centers and two visited health posts have electricity and the rest facilities use solar system as source of electricity for refrigerators. All visited health centers and the woreda health office have desktop computers with eHMIS software, printers, motorcycles and telephone service. The surveillance system lacks materials and equipment's like generators, IEC materials and projectors.

Surveillance System Attributes

Usefulness:

All health facilities accepted that the surveillance system is very useful to detect outbreaks, determine magnitude of morbidity and mortality, evaluate the effectiveness of malaria

prevention and control programs. The respondents confirmed that the surveillance system is helpful for early case detections and take actions to prevent and control epidemics. Malaria trend analysis was made in Woreda health office and all health centers to detect epidemic which shows weekly count of malaria cases and epidemic threshold which is posted. However, those health centers didn't update their monitoring chart every week, so that they are not able to detect an epidemic.

Simplicity:

All respondents in the assessed health facilities responded, the case definition of malaria (both standard and community) is simple and easy to understand. Community case definitions which is prepared by local languages is easy to be used by those who can't read English particularly health extension workers and community health workers at village level. The reporting formats being used are also very easy to understand. An average time to fill formats took less than 10 minutes for health facilities. Data collected at Woreda level by paper based then need to be converted to electronic form for documentation, as a result it took relatively long time at woreda health office.

Flexibility:

All visited Health Office and Health Facilities declared that the currently used reporting formats and procedures were flexible and could accommodate other newly occurring health events (diseases) without much difficulty and are easy to integrate with other systems and the formats were said to be easy and comprehensive to record and report. This is due to the availability of a blank column for others. It is also easy to use new technologies.

Acceptability:

The engagement of the reporting agents was very satisfactory and the reporting rate of all health facilities were 100% over the past 21 epi reporting weeks. The case definition and reporting tools were acceptable by all stakeholders. All Governmental reporting agents were 6 Health Centers and 19 Health Posts respectively have accepted and have been engaged in the surveillance system unless they are busy with other competing activities.

Representativeness:

In the district all rural Kebeles has their own functional health post and the population under surveillance at each kebele is below 5,000. The population has good health seeking behavior for the disease. The surveillance system has the capacity to pick all public health emergencies in the community. However, the weekly reporting formats lack some important variables like age (only incorporated less than 5 and above 5 year), sex and other possible risk factors.

Sensitivity:

All health centers reported that the malaria case definition used now can pick every malaria cases correctly. The community case definition helps particularly the health extension workers (HEWs), and community health workers (CHWs) to identify and notify all suspected malaria cases early at the community level.

Predictive Value Positive:

the positive predictive value of the woreda for this year is 13.3% and in comparison, with the previous year (19.2%), it is decreased by 44.36%.

Years	Total cas Tested for malaria	Malaria Treated case				Positivity rates/%/
		PF	PV	Clinical malaria	Total	
2006	194	16	24	0	40	20.6
2007	92	15	17	0	32	34.8
2008	410	73	64	0	137	33.4
2009	591	43	45	0	88	14.9
2010	506	54	43	0	97	19.2
2011	195	11	15	0	26	13.3

Figure 2: Positive predictive value of malaria cases from 20011-2014 EFY, Ankober, Ethiopia

Timeliness:
The surveillance report timeliness of the district in 2022was 97%.

Completeness:
The Woreda surveillance report completeness in 2022 was 100%.

Stability:
All health facilities responded that data were collected by their own phone call and officers didn't get refilled their expenses and also staff turnover and lack of resources had affected surveillance activities. When trained surveillance personnel and focal persons leave the position there will be difficulties in data collection and reporting.

DISCUSSION

In all assessed Health Facilities, there were available and posted standard and community case definition of the majority reportable diseases including malaria which is in line with surveillance evaluations done in Enderta, Tigray and halaba special woreda, SNNPR(18,19) but it was not actually used at the visited health posts and didn't enhances the case detection contrary to the study done in Adama town, Oromia and Enderta, Tigray Region(18,20). Malaria is the one of disease in the country which can be diagnosed and treated by health extension workers at health post level but in all visited health posts, malaria is not diagnosed and treated rather than referring to nearby HCs in Ankober woreda. The visited facilities lack case investigation form, line list, case-based forms and daily epidemic reporting format, but these formats are commonly found in other malaria elimination targeted woredas like lasta and lalibela woredas.

Ankober woreda PHEM core process reported 26 total confirmed malaria cases (11 PF and 15 PV) among 195 suspected cases of malaria and zero deaths among all age groups in 2014 EFY which is confirmed by the eHMIS data. The reported case is low and insignificant and the number of plasmodium falciparum is lower than vivax in contradiction to woredas not targeted for elimination like halaba special woreda and Adama town, Oromia(19,20). Lack of diagnostic materials like RDT in health posts make difficult for diagnoses and treatment difficult at health post level as deviated from the study in adama, Oromia. Contacts of malaria cases screening and investigation not done and there is no either paper based or electronic patient registry in all visited health posts in line with the study done in south east parts of Tigray for electronic based but deviated on paper based. Data analysis by time were done irregularly for trend analysis but analysis by place and person, creating frequency tables, calculating rates, and plotting simple graphs was poor like most of the woredas in the country.

The Malaria surveillance system presented in all assessed health institutions was able to determine the magnitude of the disease for planning and intervention as the overall completeness and timeliness of the woreda for 2022 were 100% (21rep/21wk) and 97% respectively, which is above the minimum requirement recommended by WHO. Even though frequent training is mandatory for sustainable and stable surveillance system, officers who did have a training on relevant areas in 2014 EFY is very low as compared to the study done in Asagirt and this is due to high staff turnover. Written feedback was given to two assessed health centers from Woreda health office PHEM Core Process with evidence of sample reports but there is inconsistencies and oral feedback is given to most health facilities on irregular bases, which is not appropriate form of giving feedback and not trusted during system evaluation since there is no evidence of giving feedback like written ones.

Emergency preparedness and response plan were prepared in the Woreda health office supported by malaria emergence budget. However, in case of experiencing any emergency other than malaria, the Woreda will mobilized the budget for response activity that may affect the preparedness level during times of outbreaks. Rapid Response Team is found in the woreda and epidemic management committee in the health centers but they need to have a regular meeting for discussing and anticipating public health emergencies and need to have a written documents confirming the presence of the committee. Lack of RDT kit for malaria in health posts obliged HEWs to refer suspected cases to nearby HC. Most surveillance system attributes are good like the study in Enderta, Tigray and Adama but the stability of the system is in misfortune. Mobile card expense for reporting were found to be very challenging and surveillance officers are complaining for, there is no refunding for the expense. Working surveillance as an additional job and reduced training opportunity added with poor incentive mechanism may make low motivation and satisfaction with their job that definitely did affect the surveillance activities and subsequently affect the stability of the system. Contrary to this finding, the study in Enderta confirmed that, officers working in surveillance and epidemic management had got 100 birr per month for mobile charging and frequent training opportunities (18).

Positive predictive value is low (13.3%) as compared with the study in Enderta, Tigray PPV (36%), which indicates many of the detected cases are not true cases, may be due to less specific case definition or highly sensitive case definition used but it is expected using sensitive case definitions to capture all cases of malaria. Health seeking behavior of the community for malaria were found to be good especially urban community, which is a good opportunity for active surveillance and subsequently for elimination of malaria.

CONCLUSION

The Malaria surveillance system presented in all assessed health institutions of Ankober woreda was found to be able to determine the magnitude of the disease for planning and intervention and detect change in malaria mortality and morbidity as the overall completeness and timeliness of the woreda for 2022 were 100% (21rep/21wk) and 97% respectively, which is above the minimum requirement recommended by WHO. Malaria surveillance system were also found to be satisfactory to achieve the intended objective of surveillance for public health action. It is useful, simple, flexible, acceptable, sensitive, and representative to all surveillance officers but not stable. Transmission of malaria in the woreda is found to be low and burden of the diseases is insignificant. Timeliness and completeness of report was found to be very good but for the satisfactory result of the surveillance system, the positive predictive value (13.3%) should be improved.

RECOMMENDATION

- Surveillance data should be analyzed regularly by place, person and time at all level and interpreted for public health action.
- Regular training and workshop on malaria surveillance and surveillance-related activities is required for human resource skill build up, since the woreda is in elimination phase.
- Political commitment and leadership should take ownership of EPRP implementation
- Health facilities should prepare their own EPRP
- Different reporting formats, RDT kits generator during times of electricity off, and projectors need to be in place for all health facilities
- Regular supportive supervision using checklist should be done at each level to increase the quality of the surveillance system
- The stability of the surveillance at health facility level (especially at HP) needs a special attention since they are working as an additional job.

The positive predictive value should be improved.

REFERENCES

1. Lee LM. Updated Guidelines for Evaluating Public Health Surveillance Systems Recommendations from the Guidelines Working Group. 2014;(September).

2. Calba C, Goutard FL, Hoinville L, Hendrikx P, Lindberg A, Saegerman C, et al. Surveillance systems evaluation : a systematic review of the existing approaches. ??? [Internet]. 2015; Available from: ???

3. National A, State R, Bureau H, Agency C. Amhara National Regional State Health Bureau Ethiopia , Amhara Region Infectious Disease Surveillance (AmRids) Project Completion Report. 2015;(February).

4. Choi BCK. The Past , Present , and Future of Public Health Surveillance. 2012;2012(Table 1).

5. Surveillance CD. World Health Organization.

6. Public Health Emergency Management. 2012;

7. World malaria report 2018. 2018.

8. Box PO. Current Status of Malaria in Ethiopia : Evaluation of the Burden , Factors for Transmission and Prevention Methods. 2018;7(1):1–6.

9. Malaria surveillance, monitoring & evaluation: a reference manual.

10. Guidelines F. Overview of Evaluating Surveillance Systems. 2013;

11. Vajda ÉA, Webb CE. Assessing the Risk Factors Associated with Malaria in the Highlands of Ethiopia : What Do We Need to Know ? 2017;1–13.

12. Alaria in.

13. Ibrahim BS, Abubakar AA, Bajoga UA. Evaluation of the Malaria Surveillance System in Kaduna State , Nigeria 2016 ISDS 2016 Conference Abstracts Evaluation of the Malaria Surveillance System in Kaduna State , Nigeria 2016. 2016;(May 2017):2016–8.

14. Leader T. WHO Malaria Surveillance Reference Manual. 2018;(May).

15. Jima D, Wondabeku M, Alemu A, Teferra A, Awel N, Deressa W, et al. Analysis of malaria surveillance data in Ethiopia : what can be learned from the Integrated Disease Surveillance and Response System ? Malar J

[Internet]. 2012;11(1):1. Available from: Malaria Journal

16. Report MW. Malaria Surveillance — United States , 2015. 2018;67(7).

17. WHO, diseases surveillance for malaria elimination, An operational manual, Geneva, 2012 available at *(http://www.who.int/about/licensing/copyright_form/en/index.html).*

18. Mesfin A. Addis Ababa University , College of Health Sciences , School of Public Health. Evaluation of surveillance system in South East zone, Enderta Woreda Tigray regional sate, Ethiopia, 2016;

19. Hailu E. Addis Ababa University , College of Health Sciences , School of Public Health Ethiopian Field Epidemiology and Laboratory Training Program (EFETP). Evaluation of Malaria Surveillance System in Halaba Special Woreda, Southern Nations, Nationalities and People Region, 2015

20. Taye G. Evaluation of malaria and measles surveillance system in Adama town, Oromia Region, 2017;

Applied Sciences Research Periodicals – ISSN 3033-330X
March 2024, Vol. 2, No. 3, pp. 22-27

Risk Factors for Hormone-Dependent Tumors: Breast and Prostate Cancer

Doepp, Manfred

1. HolisticCenter, 13 Haupt St., Abtwil 9030, Switzerland

Abstract:
It is a fact that gender- and hormone-dependent cancers are on the rise. This is no coincidence, but is due to a number of risk factors. These include: relative predominance of estrogens, xeno-estrogens especially in drinking water, intoxication by hydrocarbons and metals, radiation exposure, consequences of mRNA vaccinations, inadequate laboratory diagnostics with excessive normal ranges. Normal hormone levels in the blood should be aimed for individually; biochemical castration is an inadequate alternative. In order to avoid the negative developments, there is a selection of natural or nature-identical remedies (e.g., prohormones), which are listed below.

INTRODUCTION

The types of cancer dependent on sex hormones are increasing. (1) At the same time, the fertility rate in civilized countries is decreasing, e.g. the number of sperm per ejaculate, and the number of births per year is also falling. (2) The frequency of premature births and miscarriages is increasing. The erectile potency of men, on the other hand, decreased. It could be assumed that something has changed for the worse in the area of sex hormones in recent years. There are several possible explanations for this, which are listed here.

RISK FACTORS FOR BOTH SEXES

Elevated oestrogen levels in the blood (relative to the individual norm, depending on gender and age) are disadvantageous for both sexes. Estrogen receptor-positive cancers predominate in women, far more than progesterone-dependent cancers. Although an elevated estrogen level alone will not cause cancer, it will in conjunction with other risk factors. In men, increased estrogen levels are already visually recognizable by the growth of the breasts. The cause lies in the competition between the metabolism of estrogen in the liver and the breakdown of ethanol, especially in the presence of steatosis hepatis. In some countries, fatty liver has already achieved the status of a widespread disease, partly due to the generally increased consumption of ethanol and partly due to the passage of fusel alcohols (e.g., methanol) from the small intestine into the liver in the presence of intestinal dysbiosis and maldigestion. (3)

XENOESTROGENS

The most important risk factor today for both sexes are xenoestrogens. They are synthetically produced chemical compounds with an estrogen-like effect on the hormone system of an organism and are therefore classified as endocrine disruptors. (4, 5) They are distinguished from phytoestrogens (substances with an estrogen-like effect from plants) and the pharmacologically used artificial estrogens. (6)

Wikipedia (7) : " Xenoestrogens are a type of xenohormone that imitates estrogen. They can be either synthetic or natural chemical compounds. Synthetic xenoestrogens include some widely

used industrial compounds, such as, PCBs, BPA, Teflon, and phthalates, which have estrogenic effects on a living organism even though they differ chemically from the estrogenic substances produced internally by the endocrine system of any organism. Xenoestrogens are also called "environmental hormones" or "EDC" (Endocrine Disrupting Compounds). Most scientists that study xenoestrogens, including The Endocrine Society, regard them as serious environmental hazards that have hormone disruptive effects on both wildlife and humans. The overall mechanism of action is binding of the exogenous compounds that mimic estrogen to the estrogen binding receptors and cause the determined action in the target organs."

Xenoestrogens originate in part from the degradation products of chemical therapeutics used in humans, such as birth control pills and cytostatics. (8, 9) They leave the body via the urine and can only be intercepted to a small extent by water purification plants. They pass into the drinking water and are thus absorbed (10). The leading substances in drinking water contamination are PFAS (per- and polyfluorinated alkyl substances). (11) They can even be detected in the Antarctic and are practically non-degradable.

A further proportion of xenoestrogens are formed as degradation products of fungicide and herbicide applications in agriculture, e.g. atrazine, DDT, dioxin, glyphosate, etc. They enter the groundwater and thus the drinking water. They leach directly into the groundwater and thus into drinking water. Although some of them are banned, their presence in groundwater and lakes can still be detected for a long time.

Problematic target organs are the hormone-dependent organs: breasts in women and prostate in men. This makes them the most important cancer triggers and risk factors. (12, 13, 14, 15) The purification of drinking water has become a necessity.

THE ROLE OF SEX HORMONES

Both sexes have and need all three types of sex hormones: Estrogens, gestogens and androgens. The concentrations depend on gender, age and, in women, the menstrual cycle. If we take average laboratory values, we can assume à normal ratio of 15 : 5 : 1 for women and a ratio of 1 : 2 : 15 for men. The three sex hormone types should therefore be within their own normal range on the one hand, and the ratio to each other should be within the norm on the other. If there are significant deviations from the normal ranges, there is a risk of developing a hormone-dependent cancer.

The strongest effect is an absolute and/or relative increase in estrogen in both sexes. In line with this logic, antiestrogens are used for female estrogen receptor-positive tumors. Selective estrogen receptor modulators (SERMs) are active substances that mediate their effect via estrogen receptors. (16) They belong to the group of antiestrogens and are used as drugs.

The selective estrogen receptor modulators (16) are chemically different compounds that do not have a steroid structure like estrogens. They include clomiphene, raloxifene, tamoxifen, toremifene, bazedoxifene, lasofoxifene and ormeloxifene. These substances are used in the treatment of breast cancer, osteoporosis and endometriosis.

It has been known for some time that the substances used do not inhibit all estrogen receptors. A distinction is made between alpha-type (ERα) and beta-type (ERβ) estrogen receptors. The ERα receptors are found in the breast, uterus, pituitary gland and hypothalamus. The ERβ receptors,

on the other hand, are found in the bones, blood vessels, hippocampus and higher centers of the central nervous system. Raloxifene, for example, inhibits the ERα receptors and at the same time stimulates the ERβ receptors, so that breast cancer growth is inhibited without neutralizing the protective estrogen effect on the bones. This is why they are called selective estrogen receptor modulators. (16)

For prostate tumors, however, antiandrogens ("biochemical castration") are used. (17) Antiandrogens are drugs that inhibit the effect of male sex hormones. Substances such as cyproterone acetate (6-chloro-1α,2α-methylene-17-acetoxy-pregna-4,6-diene-3,20-dione) and flutamide block androgen receptors, e.g., on the prostate, and thus neutralize the effect of androgens. This is why antiandrogens are used for prostate cancer, among other things, on the assumption that the androgen effects would promote tumor growth. Possible side effects include male breast growth (gynecomastia), loss of libido and potency (18, 19, 20, 21, 22, 23, 24, 25).

The logic here is strange. It stems from the assumption that testosterone can trigger prostate cancer. This is wrong from a naturopathic point of view, as increased estrogens are responsible for this. Conversely, a lack of testosterone is a cancer risk. Instead, it would make sense to bring all three sex hormone types into the individual norm in order to reduce the risk of cancer or cancer growth. As artificial hormones should generally not be used, the prohormones of the steroid hormones are suitable for this purpose: DHEA, 7-keto-DHEA and pregnenolone. They are effective agents for the prophylaxis and treatment of hormone-dependent tumors. The basic principle should be regular: healthy and desirable is not a hormone value of zero, but an adjustment to the individual normal range.

TOPIC : STANDARD RANGES IN THE LABORATORY

If you look at the standard ranges of the sex hormones, you will see that they are much too broad. This is due on the one hand to insufficient individualization and on the other hand to the fact that the selection of test subjects is too generous. It would be necessary to aim for and use a "supernormal normal population" with narrower norm ranges. When using the usual normal ranges, it is difficult to identify potential dysfunctions or calculate adequate relationships between the three types.

EJACULATIONS

All organs in the body have the desire to function well according to their function. Shutting them down is always unphysiological and harmful. With regard to the mammary glands and the prostate, this also includes age-appropriate sexuality, in principle without age limits. If this is not possible within the framework of a partner relationship, masturbation should be used as a substitute. A social devaluation of this is not indicated. The prostate likes to be emptied again and again instead of having its contents accumulate. If its contents accumulate, the risk of prostatitis caused by chlamydia or trichomonads is increased. In chronic cases, the risk of malignant degeneration increases.

SPIKE PROTEINS

Since the coronavirus pandemic and the mRNA vaccinations, many people have had dangerous spike proteins in their bodies. (26, 27) They dock onto all organs that have ACE 2 and similar receptors. This primarily affects the myocardium and the brain, but also hormone-dependent organs. It is therefore not surprising that so-called turbo-cancers occur. Increased DNA breaks occur in the cell nuclei and mitochondria, which have to be repaired by intracellular enzymes.

These can be administered orally. (28) Neutralizing antibodies against spike proteins are important. The patient himself can use quercetin, dandelion juice and pine needle extract.

INTOXICATIONS

Metals are only partly necessary in the body, but both light metals (aluminum, titanium, etc.) and heavy metals (lead, mercury, platinum, palladium, cadmium, etc.) are dangerous. Hormonally active organs preferentially absorb such metals and they can act as cancer triggers. Detoxification, e.g. with chelates, should be carried out. Artificial hydrocarbons and micro- and nanoplastic particles are further potentially carcinogenic toxins.

RADIATION EXPOSURE

Ionizing radiation is known to cause cancer. This is generally recognized. Nevertheless, they are used too frequently, especially in cancers patients. In addition, there is growing evidence that non-ionizing radiation at high intensities can also cause cancer. Cancer therapists should be aware of this.

DIAGNOSIS

This should be as non-invasive as possible. Under no circumstances should there be any spread of possible cancer cells into the surrounding tissue, blood or lymphatic system. To this end, a) exerting pressure on the organs, b) exposing the organs to radiation, c) biopsies (punched or even fan-shaped), d) trial excisions should be avoided. The following should be used primarily for diagnosis: a) sonography, b) magnetic resonance imaging (MRI), c) tumor markers.

NATURAL REMEDIES

Natural remedies can be used to strengthen the prostate and increase a man's libido. Ingredients include: L-Arginine, Tribulus terrestris, Maca, Red Ginseng, Cordyceps chin, Cinnamomum cassia, Dioscorea opposita, Coix Lacryma-Jobi, Cuscuta chin, Ganoderma lucidum, Schisandra chin, Ziziphus Giuggiola, Atractylodes macrocephala, Lycium chin.

Appropriate remedies for women may include: Fenugreek seeds, Ashwagandha, Muira puamana, Saffron, Cordyceps chin, Reishi/Ling Zhi. This makes it possible for both sexes to lead a more satisfying partner life and prevent cancer.

SUMMARY

We are not at the mercy of negative developments in the incidence of cancer, but can take preventive measures if we are aware of the risk factors. This includes, among other things: Purification of drinking water, increasing progesterone in women and testosterone in men, cure detoxification, avoidance of radiation exposure, avoidance of artificial chemical hormones, avoidance of harmful diagnostic effects, neutralization of spike proteins.

REFERENCES

1. https://tkp.at/2023/03/15/vaers-daten-belegen-turbokrebs-6-metastasen-und-uebersicht/

2. https://www.destatis.de/DE/Themen/Gesellschaft-Umwelt/Bevoelkerung/Geburten/geburten-aktuell.html

3. https://www.deutsche-leberstiftung.de/presse/pressemappe/lebererkrankungen/fettleber/nicht-alkoholische-fettleber/

4. R. Viñas, Y. J. Jeng, C. S. Watson: Non-genomic effects of xenoestrogen mixtures. In: International journal of environmental research and public health. Vol 9, No 8, August 2012, pp. 2694-2714, doi :10.3390/ijerph9082694. PMID 23066391. PMC 3447581

5. Paterni, Ilaria; Granchi, Carlotta; Minutolo, Filippo (2017-11-02). "Risks and benefits related to alimentary exposure to xenoestrogens". Critical Reviews in Food Science and Nutrition. 57 (16): 3384-3404. doi:10.1080/10408398.2015.1126547. ISSN 1040-8398. PMC 6104637. PMID 26744831

6. Wang, Xiaoqiang; Ha, Desiree; Yoshitake, Ryohei; Chan, Yin S.; Sadava, David; Chen, Shiuan (2021-08-16). "Exploring the Biological Activity and Mechanism of Xenoestrogens and Phytoestrogens in Cancers : Emerging Methods and Concepts". International Journal of Molecular Sciences. 22 (16): 8798. doi:10.3390/ijms22168798. ISSN 1422-0067. PMC 8395949. PMID 34445499

7. https://en.wikipedia.org/wiki/Xenoestrogen

8. Statement from the work session on environmental endocrine-disrupting chemicals: neural, endocrine, and behavioral effects". Toxicology and Industrial Health. 14 (1-2) : 1-8. 1998. bibcode :1998ToxIH.14.1. doi :10.1177/074823379801400103. PMID 9460166. S2CID 45902764

9. Mueller SO (February 2004). "Xenoestrogens: mechanisms of action and detection methods". Analytical and Bioanalytical Chemistry. 378 (3) : 582-587. doi :10.1007/s00216-003-2238-x. PMID 14564443. S2CID 46507842

10. Aravindakshan J, Paquet V, Gregory M, Dufresne J, Fournier M, Marcogliese DJ, Cyr DG (March 2004). "Consequences of xenoestrogen exposure on male reproductive function in spottail shiners (Notropis hudsonius)". Toxicological Sciences. 78 (1) : 156-165. doi :10.1093/toxsci/kfh042. PMID 14657511

11. "Poison in Swiss drinking water, every second water sample contained unhealthy chemicals." Ktipp No 12, June 21, 2023, pp 12-13

12. Acerini CL, Hughes IA (August 2006). "Endocrine disrupting chemicals: a new and emerging public health problem?". Archives of Disease in Childhood. 91 (8): 633-641. doi:10.1136/adc.2005.088500. PMC 2083052. PMID 16861481.

13. Patisaul HB, Adewale HB (2009). "Long-term effects of environmental endocrine disruptors on reproductive physiology and behavior". Frontiers in Behavioral Neuroscience. 3: 10. doi:10.3389/neuro.08.010.2009. PMC 2706654. PMID 19587848.

14. Degen GH, Bolt HM (September 2000). "Endocrine disruptors: update on xenoestrogens". International Archives of Occupational and Environmental Health. 73 (7) : 433-441. bibcode :2000IAOEH..73..433D. doi:10.1007/s004200000163. PMID 11057411. S2CID 24198566.

15. Stradtman SC, Freeman JL (August 2021). "Mechanisms of Neurotoxicity Associated with Exposure to the Herbicide Atrazine". Toxics. 9 (9): 207. doi:10.3390/toxics9090207. PMC 8473009. PMID 34564358.

16. Riggs, B.L. & Hartmann, L.C. (2003): Selective estrogen-receptor modulators -mechanisms of action and application to clinical practice. In: N. Engl. J. Med. vol. 348, pp. 618-629. PMID 12584371

17. Amelung T1, Kuhle LF, Konrad A, Pauls A, Beier KM.: Androgen deprivation therapy of self-identifying, help-seeking pedophiles in the Dunkelfeld. In: International Journal of Law and Psychiatry. Vol 35, No 3, May 2017, PMID 22420933

18. Robert Koch Institute (RKI), prostate diseases. GBE issue 36, 2007

19. EAU Guidelines on Prostate Cancer. Eur Ass Urology (2015); www.uroweb.org

20. S3 guideline prostate cancer. October 2014, AWMF-Register-Number 043/022OL

21. Hager, B., et al, Integrated prostate cancer centers might cause an overutilization of radiotherapy for low-risk prostate cancer : A comparison of treatment trends in the United States and Germany from 2004 to 2011. Radiotherapy and Oncology, Vol 115 (2015) 90-95, doi: 10.1016/j.radonc.2015.02.024.

22. Professor Dr. Bertrand Tombal from Saint-Luc Hospital, Brussels, Belgium, statement at the European Cancer Conference ECC 2015 in Vienna.

23. Rothamel, M., et al, Significant change in therapy. Uro-News 18 (2014) 2-5.

24. James et al, STAMPEDE study, http://abstracts.asco.org/156/AbstView_156_147721.html

25. Professor Dr. Jürgen Breul, Loretto Hospital, Freiburg : "New treatment options for patients with castration-resistant prostate cancer", lecture at the 14th Pharmaceutical Oncology Congress NZW-Munich 2015

26. https://www.rki.de/DE/Content/InfAZ/N/Neuartiges_Coronavirus/Virologische_Basisdaten.html

27. https://flexikon.doccheck.com/de/Spikeprotein

28. www.citozeatecsrl.ch

Applied Sciences Research Periodicals – ISSN 3033-330X
March 2024, Vol. 2, No. 3, pp. 28-50

The Disenchantment in Modern Physics

Wim Vegt

1. Department of Physics, Eindhoven University of Technology, The Netherlands

Abstract:
Isaac Newton looms over the Enlightenment as the giant who steered humanity out from under the dark shadows of superstition and into the bright, sterile light of the mechanical universe. Armed with the navigational tools of empirical evidence and mathematical proofs, he deciphered the forces of nature using human reason alone. With the publication of his masterwork Principia in 1687, the archaic belief in Nature's soul was left shipwrecked on the shores of the unscientific past. Newton's legacy is scientific positivism, or the belief that an idea is true only when it can be proved mathematically. If, in collective memory, René Descartes (1596-1650) succeeded in splitting the mind from the body, then Newton's clockwork universe desacralized nature and cleaved the body from the soul. [43] At the end of 1918, Max Weber proclaimed at the University of Munich that 'the fate of our times' is the 'disenchantment of the world' The understanding that mystery and sacredness was disappearing from a world increasingly dominated by industry, science, and technology had its intellectual roots in German Romanticism, where it had found expression in the works of Novalis and Friederich Hölderlin. After Weber reintroduced the evocative term, "Entzauberung", it would go on to have a deep impact on theories of modernity developed by the following generations.[44] Newton dressed his mystical intuition in mathematical proofs before presenting his ideas to the world. The father of mechanical science believed that spirit animated matter and his work was to understand, using the gifts of his meager human intellect, the eternal and divine. This article focusses on the "Prima Materia" described by Isaac Newton [43] and already thousands of years ago in "The Emerald Tablet of Hermes Trismegistus". [45] In the Emerald Tablet, the "One Thing" refers to the "Prima Materia". This was then acted upon by the thoughts or word of the One Mind to create the material reality we can observe with our senses. The fundamental concept of the "Prima Materia"" has been expressed in Equation (16) and (17) in which" Light" is the "Prima Materia" of our reality and the origin of our universe. Light is the building material out of which this universe has been created. The new theory, describing electro-magnetic-gravitational-acceleration force density interactions (expressed in N/m3), has been discussed at astronomical levels: Gravitational RedShift, Black Holes and Dark Matter and at sub-atomic levels: The absorption and emission of light at sub-atomic levels in concentric spheres by an atom at discrete energy levels. Evidence will be demonstrated about the correctness of this new electro-dynamic theory which represents the only theory which connects electro-dynamics in a correct way with plasma-dynamics. In general, the gravitational (acceleration) force densities, originating from rotation and linear accelerations, are being ignored but with nuclear fusion processes these gravitational (acceleration) forces become fundamental and are necessary to develop a stable nuclear fusion process. Differently than in General Relativity, the electro-magnetic-gravitational-acceleration force density interactions (expressed in N/m3) [35] fundamentally has been based on the divergence of the sum of the "Stress Energy Tensor" and the introduced "Gravitational-Acceleration" Tensor. The theory describes "Gravitational-Acceleration-Electromagnetic" Interaction resulting in a mathematical Tensor presentation for BLACK HOLEs. (**G**ravitational **E**lectr**o**magnetic Co**n**finements) [1] The

"Electromagnetic Energy Gradient" creates a second order effect "Lorentz Transformation" which results in the Gravitational Field of BLACK HOLEs which determines the interaction force density between the confinement of Light (BLACK HOLE's) and the "Gravitational-Acceleration" Field. Einstein approached the interaction between gravity and light by the introduction of the "Einstein Gravitational Constant" in the 4-dimensional Energy-Stress Tensor $\varkappa T_{\mu\nu}$(1) In this alternative approach related to General Relativity, the interaction between gravity and light has been presented by the sum of the Electromagnetic Tensor $T_{\mu\nu}$ and the "Gravitational-Acceleration" Tensor $J_{\mu\nu}$(2) The new theory describes the impact of "CURL" [38] within the gravitational fields around Black Holes and the impact on Gravitational Lensing. Gravitational "CURL" (Equation 6) is an effect which cannot be explained and calculated by General Relativity. The new approach presents mathematical solutions for the BLACK HOLEs (**G**ravitational **E**lectr**o**mag**n**etic Interaction) introduced in 1955 by Jonh Archibald Wheeler in the publication in Physical Review Letters in 1955 [1]. The mathematical solutions for BLACK HOLEs are fundamental solutions for the relativistic quantum mechanical Dirac equation (Quantum Physics) in Tensor presentation (41). Assuming a constant speed of light "c" and Planck's constant ħ within the BLACK HOLE, the radius "R" of the BLACK HOLE with the energy of a proton, is about 1% of the radius of the hydrogen atom (14). The New Theory has been tested in an experiment with 2 Galileo Satellites and a Ground Station by measuring the Gravitational RedShift in a by the Ground Station emitted stable MASER frequency [2]. The difference between the calculation for Gravitational RedShift, within the Gravitational Field of the Earth, in "General Relativity" and the "New Theory" is smaller than 10^{-16} (12) and (13). In all "General Redshift Experiments" "General Relativity" and the New Electrodynamic-Gravitational-Acceleration" Theory predict a Gravitational RedShift with a difference smaller than 15 digits beyond the decimal point which is beyond the accuracy of modern "Gravitational Redshift" observations. Both values are always within the measured Gravitational RedShift in all observations being published since the first observation of the gravitational redshift in the spectral lines from the White Dwarf which was the measurement of the shift of the star Sirius B, the white dwarf companion to the star Sirius, by W.S. Adams in 1925 at Mt. Wilson Observatory. Theories which unify Quantum Physics and General Relativity [32], like "String Theory", predict the non-constancy of natural constants. Accurate observations of the NASA Messenger [11] observe in time a value for the gravitational constant "G" which constrains until ($|\dot{G}|$ /G to be < 4×10^{-14} per year). One of the characteristics of the New Theory is the "Constant Value" in time for the Gravitational Constant "G" in unifying General Relativity and Quantum Physics.

Keywords: Quantum Physics, General Relativity, Gravitational RedShift, Black Holes, Dark Matter, Nuclear Fusion, Nuclear Plasmas.

AN ALTERNATIVE APPROACH IN GRAVITY AND ACCELERATION

Einstein approached the interaction between gravity and light by the introduction of the "Einstein Gravitational Constant" in the 4-dimensional Energy-Stress Tensor.

$$G_{\mu\nu} + \Lambda\, g_{\mu\nu} = \kappa\, T_{\mu\nu} \tag{1}$$

In which $G_{\mu\nu}$ equals the Einstein Tensor, $g_{\mu\nu}$ equals the Metric Tensor, $T_{\mu\nu}$ equals the Stress-Energy tensor, Λ equals the cosmological constant and $\varkappa$ equals the Einstein gravitational constant.

An alternative approach to Einstein's expression with the tensor $\varkappa T_{\mu\nu}$, describing the curvature of the Space-Time continuum, is the sum of the Electromagnetic Tensor $T_{\mu\nu}$ and the "Gravitational-Acceleration" Tensor$J_{\mu\nu}$.

$$\kappa \, \mathrm{T}_{\mu\nu} \;\Leftrightarrow\; \mathrm{T}_{\mu\nu} \;+\; \mathrm{J}_{\mu\nu} \tag{2}$$

The 4-dimensional divergence of the sum of the Electromagnetic Stress-Energy tensor and the Gravitational Tensor expresses the 4-dimensional Force-Density vector (expressed in [N/m^3] in the 3 spatial coordinates) as the result of Electro-Magnetic-Gravitational interaction.

$$f^{\mu} \;=\; \partial_{\nu} \left(\mathrm{T}^{\mu\nu} + \mathrm{J}^{\mu\nu} \right) \tag{3}$$

In vector notation the 4-dimensional Force-Density vector can be written as:

$$\overline{f}^{4} = \begin{pmatrix} f_4 \\ f_3 \\ f_2 \\ f_1 \end{pmatrix} = \square \, \square \left(\overline{\overline{\mathrm{T}}} + \overline{\overline{\mathrm{J}}} \right) \tag{4}$$

The fundamental boundary condition for this alternative approach to gravity is the requirement that the Force 4 vector equals zero in the 4 dimensions, expressing a universal 4-dimensional equilibrium:

$$\overline{f}^{4} = \begin{pmatrix} f_4 \\ f_3 \\ f_2 \\ f_1 \end{pmatrix} = \square \, \square \left(\overline{\overline{\mathrm{T}}} + \overline{\overline{\mathrm{J}}} \right) = \overline{0}^{4} \tag{5}$$

The 3 spatial components of the Force-Density vector, as a result of Electro-Magnetic-Gravitational interaction can be written as:

$$\bar{f} = -\frac{1}{c^2}\frac{\partial(\bar{E}\times\bar{H})}{\partial t} + \varepsilon_0\,\bar{E}\,(\nabla\cdot\bar{E}) - \varepsilon_0\,\bar{E}\times(\nabla\times\bar{E}) +$$

$$+\mu_0\,\bar{H}\,(\nabla\cdot\bar{H}) - \mu_0\,\bar{H}\times(\nabla\times\bar{H}) + \gamma_0\,\bar{g}\,(\nabla\cdot\bar{g}) - \gamma_0\,\bar{g}\times(\nabla\times\bar{g}) = \bar{0}\quad [N/m^3]$$

in which:

$\varepsilon_0\,(\nabla\cdot\bar{E}) = \rho_E$ Electric Charge Density $[C/m^3]$

$\mu_0\,(\nabla\cdot\bar{H}) = \rho_M$ Magnetic Flux Density $[Vs/m^3]$ or $[Wb/m^3]$

$\gamma_0\,(\nabla\cdot\bar{g}) = \rho_M$ Mass Density (Electromagnetic) $[kg/m^3]$

Electric Energy Density: $w_E = \frac{1}{2}\varepsilon_0 E^2$

Magnetic Energy Density: $w_M = \frac{1}{2}\mu_0 H^2$

Gravitational Energy Density: $w_G = \frac{1}{2}\gamma_0 g^2$

$\bar{g}$ acceleration (gravitational or mechanical/dynamical)

(6)

In which E represents the electric field intensity expressed in [V/m], H represents the magnetic field intensity expressed in [A/m] and g represents the gravitational acceleration expressed in [m/s²]. The permittivity indicated as ε_0, the permeability indicated as μ_0 and the gravitational permeability of vacuum as γ_0.

For curl-free gravitational fields equation (6) can be written as:

$$\bar{f} = -\frac{1}{c^2}\frac{\partial(\bar{E}\times\bar{H})}{\partial t} + \varepsilon_0\,\bar{E}\,(\nabla\cdot\bar{E}) - \varepsilon_0\,\bar{E}\times(\nabla\times\bar{E}) + \quad (7)$$

$$+\mu_0\,\bar{H}\,(\nabla\cdot\bar{H}) - \mu_0\,\bar{H}\times(\nabla\times\bar{H}) + \bar{g}\,\rho_M = \bar{0}\quad [N/m^3]$$

Substituting Einstein's $W = m c^2$ in (7) results in "Electro-Magnetic-Gravitational Equilibrium Field Equation" (8):

$$\bar{f} = -\frac{1}{c^2}\frac{\partial(\bar{E}\times\bar{H})}{\partial t} + \varepsilon_0\,\bar{E}\,(\nabla\cdot\bar{E}) - \varepsilon_0\,\bar{E}\times(\nabla\times\bar{E}) + \quad (8)$$

$$+\mu_0\,\bar{H}\,(\nabla\cdot\bar{H}) - \mu_0\,\bar{H}\times(\nabla\times\bar{H}) + \frac{1}{2c^2}\bar{g}\left(\varepsilon E^2 + \mu H^2\right) = \bar{0}\quad [N/m^3]$$

The theory describes "Electromagnetic-Gravitational Interaction", "Magnetic-Gravitational Interaction" and "Electric-Gravitational Interaction". In this new theory particles do not interact with fields. The interaction between an electric charged particle and an electric field is not the interaction between a particle and a field but it is the interaction between the electric field of the particle interacting with the other electric field. Every interaction is an interaction between fields. Electric Fields interact with Electric Fields, Magnetic Fields interact with Magnetic Fields and Gravitational Fields interact with Gravitational Fields.

"GRAVITATIONAL REDSHIFT/ BLUESHIFT IN "LIGHT (EMR)" DUE TO "ELECTROMAGNETIC GRAVITATIONAL INTERACTION"

To test the New Theory, the Gravitational-Redshift experiment: "Test of the Gravitational Redshift with Galileo Satellites in an Eccentric Orbit" by S. Hermann et all, has been chosen [2]. In this experiment a stable "MASER" frequency from a ground station has been emitted to 2 Galileo Satellites, measuring the frequency difference between the Ground Station and the Satellites. The frequency shift has been caused by the gravitational field of the Earth and 2 satellites has been chosen to compensate for the eccentricity of the Galileo Orbit.

Assuming a gravitational field g[z] depending on the radial direction in cartesian coordinates between the ground station and the satellites:

$$\overline{g[z]} = \left\{0{,}0,\ \frac{G\ M_{Earth}}{4\ \pi\ z^2}\right\} \tag{9}$$

In which G (G = 6.67428 10^{-11} Nm^2 / kg^2) equals the Gravitational constant, M_{Earth} the mass of the earth and r the radial distance from the centre of the earth. The mathematical solution [5] of equation (8) for plane electromagnetic waves (expressed in cartesian {x,y,z} coordinates) related to the Electric Field Intensity equals:

$$\overline{E} = \begin{pmatrix} E_x \\ E_y \\ E_z \end{pmatrix} = \begin{pmatrix} e^{-\frac{G\,M_{Eearth}\ \varepsilon_0\ \mu_0}{8\ \pi\ z}}\ h\left[\ \omega_0\ e^{-\frac{G\,M_{Earth}\ \varepsilon_0\ \mu_0}{4\ \pi\ z}\left(t\ -\ \sqrt{\varepsilon\ \mu}\ z\right)}\ \right] \\ 0 \\ 0 \end{pmatrix} \tag{10}$$

And the mathematical solution of (8) for the Magnetic Field Intensity equals:

$$\overline{H} = \begin{pmatrix} H_x \\ H_y \\ H_z \end{pmatrix} = \begin{pmatrix} 0 \\ \frac{1}{\sqrt{\varepsilon_0\ \mu_0}}\ e^{-\frac{G\,M_{Earth}\ \varepsilon_0\ \mu_0}{8\ \pi\ z}}\ h\left[\ \omega_0\ e^{-\frac{G\,M_{Earth}\ \varepsilon_0\ \mu_0}{4\ \pi\ z}\left(t\ -\ \sqrt{\varepsilon\ \mu}\ z\right)}\ \right] \\ 0 \end{pmatrix} \tag{11}$$

In which ω_0 equals the original frequency of the MASER radiation propagating in the direction of the gravitational field g[z] of the Earth in the z-direction. The exponential term demonstrates the Gravitational Redshift when the MASER radiation propagates in the direction of the Gravitational Field of the earth. The propagation speed of the Electromagnetic Radiation remains constant (the speed of light). But the amplitude of the field intensity and the frequency of the field intensity diminishes exponentially.

Calculations in Mathematica [5] demonstrate a difference between the calculation with General Relativity and the calculation with the New Theory. Choosing for the ground station a distance to the centre of the earth z_1 = 6,378,000 [m] (Radius of the Earth) and for the average distance of the ESA satellites in a Galileo orbit z_2 = 23,222,000 [m] (distance from the ESA satellite to the centre of the Earth), calculated with Mathematica, the Gravitational RedShift according General Relativity equals:

$$\Delta\,\omega_{GR} = 0.00000000004011815497097883\ [s^{-1}] \quad (12)$$

Calculated with Mathematica, the Gravitational RedShift according the New Theory, which is a solution of equation (8) equals:

$$\Delta\,\omega_{GR} = 0.00000000004011824206173742\ [s^{-1}] \quad (13)$$

Both calculated values a within the Range of the measured gravitational RedShift by the average values of both ESA satellites in the Galileo orbit

$$\Delta\,\omega_{\text{Measured}} = 0.000000000040118 \pm 2.2\ 10^{-15}\ [s^{-1}] \quad (14)$$

In [2] a factor α has been defined which presents the measured deviation α between the predicted Gravitational RedShift by General Relativity and the Measured Gravitational RedShift.

$$\alpha = \Delta\,\omega_{\text{MEASURED}} - \Delta\,\omega_{\text{GR}} = (2.2 \pm 1.6) \times 10^{-5} \quad (15)$$

A comparable factor α can be used to determine which theory (General Relativity or the New Theory) has the nearest approach to the experimentally measured data. Highly accurate measuring experiments are required with an accuracy higher than 16 digits beyond the decimal point.

BLACK HOLES

Black Holes without Singularities with Dimensions Smaller than the Diameter of the Hydrogen Atom

A second fundamental solution for equation (8) describes a **G**ravitational **E**lectr**o**magn**e**tic Confinement (BLACK HOLE) [1] within a radial gravitational field with acceleration $\bar{g}$ (in radial direction). This solution represents a Black Hole, the confinement of light due to its own gravitational field, and has no singularities. This solution for equation (8) describes Black Holes, dependent of time and radius, presenting discrete spherical energy levels, within a radial gravitational field with acceleration $\bar{g}$ (in radial direction) [14] has been represented in (16) and (17).

$$\begin{pmatrix} E_r \\ E_\theta \\ E_\varphi \end{pmatrix} = \begin{pmatrix} 0 \\ f(r)\,\mathrm{Sin}(k\,r)\,\mathrm{Sin}(\omega\,t) \\ -f(r)\,\mathrm{Cos}(k\,r)\,\mathrm{Cos}(\omega\,t) \end{pmatrix} \quad \begin{pmatrix} H_r \\ H_\theta \\ H_\varphi \end{pmatrix} = \sqrt{\frac{\varepsilon}{\mu}} \begin{pmatrix} 0 \\ -f(r)\,\mathrm{Sin}(k\,r)\,\mathrm{Cos}(\omega\,t) \\ -f(r)\,\mathrm{Cos}(k\,r)\,\mathrm{Sin}(\omega\,t) \end{pmatrix} \quad \bar{g} = \begin{pmatrix} \frac{G_1}{4\,\pi\,r^2} \\ 0 \\ 0 \end{pmatrix} \quad (16)$$

$$w_{em} = \left(\frac{\mu_0}{2}(\bar{m}\,.\,\bar{m}) + \frac{\varepsilon_0}{2}(\bar{e}\,.\,\bar{e})\right) =$$

$$f(r)^2\left((\mathrm{Sin}(k\,r)\,\mathrm{Sin}(\omega\,t))^2 + (\mathrm{Cos}(k\,r)\,\mathrm{Cos}(\omega\,t))^2 + \frac{\varepsilon}{\mu}(\mathrm{Sin}(k\,r)\,\mathrm{Cos}(\omega\,t))^2 + (\mathrm{Cos}(k\,r)\,\mathrm{Sin}(\omega\,t))^2\right)$$

In which the radial function f(r) equals:

$$f[r] = K\ e^{-\frac{G\ M_{BH}\ \varepsilon_0\ \mu_0}{8\ \pi\ r}} \tag{17}$$

G represents the Gravitational constant and M represents the total confined electromagnetic mass of the BLACK HOLE. Equation (16) presents a Standing (Confined) Electromagnetic Field Configuration with a phase shift of 90 degrees between the electric field and the magnetic field with the corresponding Nodes and AntiNodes. [13]. The solution has been calculated according Newton's Shell Theorem, resulting in the fundamental concept of the "Prima Materia" [43] Assuming a constant speed of light "c" and Planck's constant ħ within the BLACK HOLE, the radius "R" (with n = 1,2,3,4....) of the BLACK HOLE with the energy of a proton, according $W = m_{proton}\ c^2$, would be: $1.5009211 \times 10^{-10}$ [J].

$$R_{GEON} = n\ \lambda = n \left(\frac{c}{f}\right) = n \left(\frac{c}{W}\right) \hbar = 7.1865\ 10^{-26} \left(\frac{n}{W}\right) \tag{18}$$

$$R_{GEON} = n\ 3.82\ 10^{-12}\ [m]$$

Black Holes are varying from atomic dimensions with dimensions of 10^{-27} [kg], Page 39 [33] until Black Holes with dimensions of 10^{40} [kg], Page 67 [34]. At these dimensions Black Holes turn into Dark Matter. The fundamental boundary condition for the confinement of Electromagnetic radiation (BLACK HOLEs) is that the energy flow (Poynting vector) $\bar{S} = \bar{E} \times \bar{H}$ equals zero at the surcface of the confinement. This is possible at every *"90 degrees Phase Shift Surface"* (*Sphere*) between the Electric Field and the Magnetic Field.

Black Holes with a Singular Point and Large Dimensions

Fig 1 represents a Black Hole with a mass of 10^{35} [kg] and a radius of about 25 [km] controlled by a different mahgematical solution for equation (8). The radius of the Black Hole equals about 25 [km] which has been controlled by a different mathematical solution (19) for equation (8).

$$f[r] = K\ e^{\left(\frac{G\ M_{BH}\ \varepsilon_0\ \mu_0}{8\ \pi\ r}\ -\ \log[r]\right)} \quad [J / m^3] \tag{19}$$

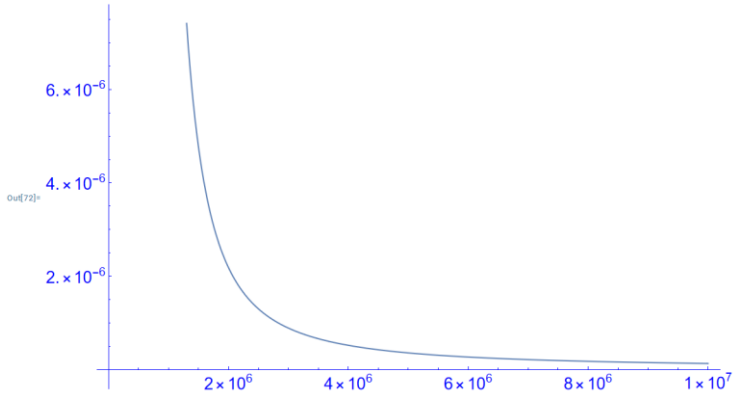

Fig. 1: The Energy Density [J/ m³] as a function of the Radius R = max 10^7 [m] of the Black Hole.

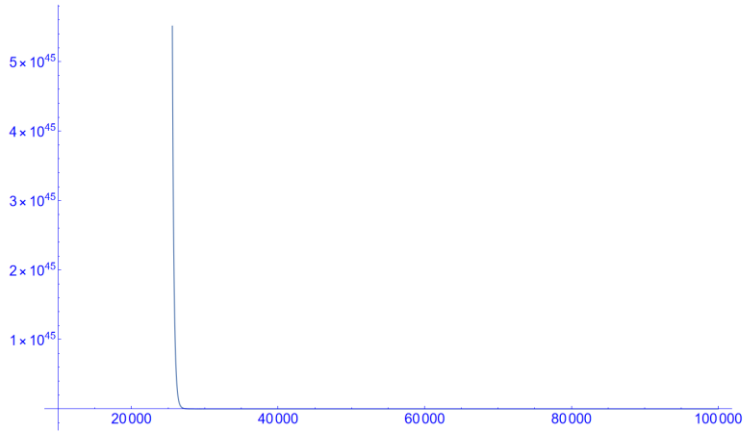

Fig. 2: The Energy Density [J/ m³] as a function of the Radius R = max 10⁵ [m]

Figure 1 and Figure 2 demonstrate the large effect of "Gravitational Intensity Shift" and "Gravitational RedShift" at the distance of 25 [km]. Over a distance of 10.000 [km] the intensity of the emitted light of the Black Hole with a mass of 10^{35} [kg] falls back with a factor of 10^{-51}. Also, the frequency of the emitted light of the Black Hole falls back with a factor 10^{-51}. Emitted light in the visible spectrum of 10^{14} [Hz] falls back to a frequency of 10^{-37} [Hz]. These extreme low frequencies with extreme low intensities have never been measured which has result in the name "Black Hole" for the phenomenon of "Gravitational Intensity Shift" and "Gravitational RedShift" for a large mass. It follows from equation (8) and the solutions (10) and (11) that the speed of light does not change inside and around Black Hole. Only the direction of the propagation of light can change due to a gravitational field.

Dark Matter in the Universe Controlled by "Gravitational Shielding"

Fig 3 represents Dark Matter with a total mass of 10^{53} [kg] and a radius of about 10 times the size of the Milky Way Galaxy. The radius of the dark mass equals 5 10^{21} [m] which has been controlled by a different mathematical solution (20) for equation (8).

$$f[r] = K\ e^{\left(\frac{G\ M_{BH}\ \varepsilon_0\ \mu_0}{8\ \pi\ r}\ -\ \log[r]\right)} \quad [J/m^3] \tag{20}$$

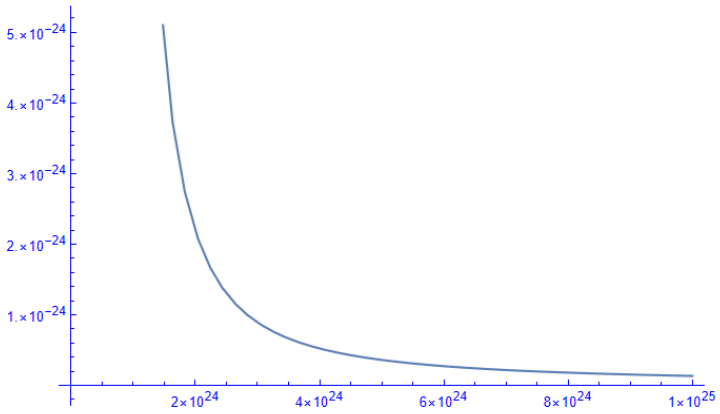

Fig. 3: The Energy Density [J/ m³] as a function of the Radius R = max 10²⁵ [m] of the Dark Matter.

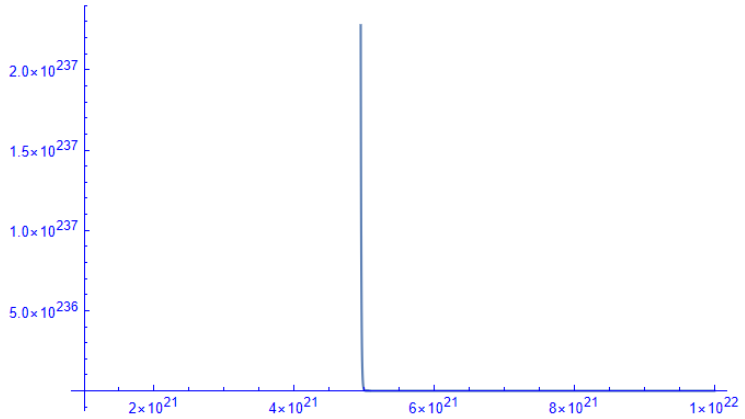

Fig. 4: The Energy Density [J/ m³] of the Dark Matter as a function of the Radius R = max 10^{22} [m]

Figure 3 and Figure 4 demonstrate the large effect of "Gravitational Intensity Shift" and "Gravitational RedShift" at the distance of 5 10^{21} [m] which is 10 times the radius of the Milky Way Galaxy. Over the distance of 5 10^{21} [m] the intensity of the emitted light of the Dark Matter with a mass of 10^{53} [kg] falls back with a factor of 10^{-261}. Also, the frequency of the emitted light of the Black Hole falls back with a factor 10^{-261}. Emitted light in the visible spectrum of 10^{14} [Hz] falls back to a frequency of 10^{-247} [Hz]. These extreme low frequencies with extreme low intensities have never been measured which has result in the name "Dark Matter" for the phenomenon of "Gravitational Intensity Shift" and "Gravitational RedShift" for an extreme large mass. It follows from equation (8) and the solutions (10) and (11) that the speed of light does not change inside and around the Dark Mass. Only the direction of the propagation of light can change due to the gravitational field of the Dark Mass.

THE RELATIONSHIP BETWEEN BLACK HOLES AND QUANTUM PHYSICS

Introducing the Quantum Vector Function $\overline{\phi}$,

$$\overline{\phi} = \sqrt{\frac{\mu}{2}} \left(\overline{H} + i \frac{\overline{E}}{c} \right) \tag{21}$$

Substituting (21) in (16) results in the quantum presentation for the BLACK HOLE:

$$\overline{\Phi(r,\theta,\varphi)} = \sqrt{\frac{\mu}{2}} \left(\overline{H} + i \frac{\overline{E}}{c} \right) f(r) \begin{pmatrix} \Phi_r \\ \Phi_\theta \\ \Phi_\varphi \end{pmatrix} \tag{22}$$

$$\overline{\Phi(r,\theta,\varphi)} = K \sqrt{\frac{\varepsilon}{\mu}}\, e^{-\frac{G1\, \varepsilon_0\, \mu_0}{8\pi r}} \begin{pmatrix} 0 & 0 & 0 \\ 0 & -\mathrm{Sin}(k\,r) & \mathrm{Sin}(k\,r) \\ 0 & -i\,\mathrm{Cos}(k\,r) & i\,\mathrm{Cos}(k\,r) \end{pmatrix} \begin{Bmatrix} 0 \\ \mathrm{Cos}\,(\omega\,t) \\ i\,\mathrm{Sin}\,(\omega\,t) \end{Bmatrix}$$

With "K" a constant value dependend of the mass of the BLACK HOLE. The Dot product between the unit vector and the Quantum Vector Function $\bar{\phi}$ represents the quantum mechanical probability function $\Psi[r,\mathrm{t}]$ which is a fundamental solution of the Schrödinger Wave Equation.

$$\overline{\Phi(r,\theta,\varphi)} = K\sqrt{\frac{\varepsilon}{\mu}}\,e^{-\frac{G1\,\varepsilon_0\,\mu_0}{8\,\pi\,r}}\begin{pmatrix}0 & 0 & 0\\ 0 & -\mathrm{Sin}(k\,r) & \mathrm{Sin}(k\,r)\\ 0 & -i\,\mathrm{Cos}(k\,r) & i\,\mathrm{Cos}(k\,r)\end{pmatrix}\begin{Bmatrix}0\\ \mathrm{Cos}\,(\omega\,t)\\ i\,\mathrm{Sin}\,(\omega\,t)\end{Bmatrix} \tag{23}$$

$$\Psi(r,t) = \begin{Bmatrix}1 & 1 & 1\end{Bmatrix}\begin{Bmatrix}0\\ \mathrm{Cos}\,(\omega\,t)\\ i\,\mathrm{Sin}\,(\omega\,t)\end{Bmatrix}K\sqrt{\frac{\varepsilon}{\mu}}\,e^{-\frac{G1\,\varepsilon_0\,\mu_0}{8\,\pi\,r}} = K\sqrt{\frac{\varepsilon}{\mu}}\,e^{-\frac{G1\,\varepsilon_0\,\mu_0}{8\,\pi\,r}}\,e^{i\,\omega\,t}$$

The Scalar function $\Psi[r,\mathrm{t}]$ represents a fundamental solution of the Quantum Mechanical Schrödinger wave equation. [36, 37]

Black Holes with Discrete Spherical Energy Levels at Sub-Atomic Dimensions

An essential requirement for the confinement of Electromagetic Energy is that the Poymtingvector equals zero at the (spherical) surface of the confinement. For the confinement within a sphere, a standing electromagnetic wave pattern has been required which exists of concentric spheres, at every sphere an antinodal plane for E (or B) with a radius distance between each sphere of half the wavelength of the confinement. The constant k = n π λ , "n" a natural number (1,2,3,4.....) and λ the wavelength.

Time and Radius Dependent Black Holes with Discrete Energy Levels, The Confinements of Electromagnetic Radiation within Spherical Regions:

Every concentric sphere represents an anti-nodal surface for the Electric Field (E) or the Magnetic Field (H).

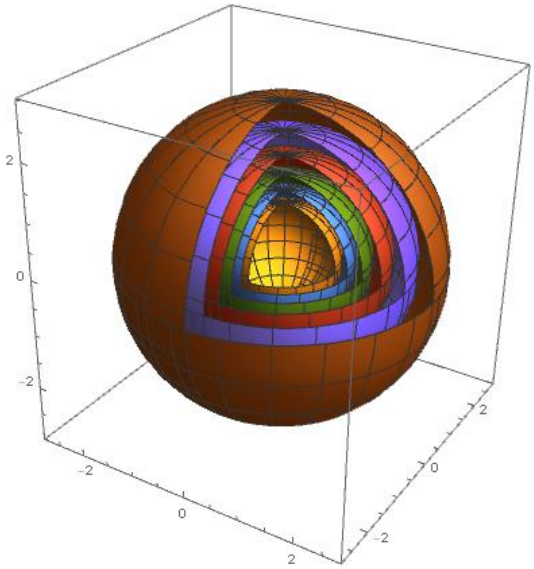

Fig. 5: Nodal and Antinodal Spheres for Standing (Confined) Spherical Electromagnetic waves with a 90 degrees phase shift between the Electric field and the Magnetic field. Equation (9)

The Poynting Vector^: $\bar{S} = \bar{E} \times \bar{H}$ at this spherical surface equals zero at any time and at any location at this sphere. The Electromagnetic Energy remains always within this sphere and the next concentric sphere. The concentric spheres have a difference in radius of one half wavelength of the electromagnetic radition within the confinement and a different discrete energy level. Every concentric sphere represents an anti-nodal suface of the electric field or the magnetic field.

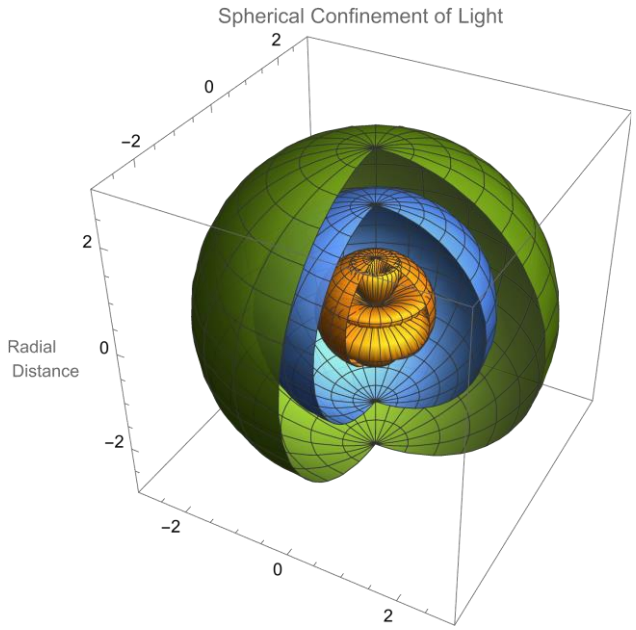

Fig. 6: Nodal- and Antinodal Spheres (k = 3) for Standing (Confined) Spherical Electromagnetic waves with a 90 degrees phase shift between the Electric field and the Magnetic field. Equation (9)

Equation (24) describes a Time and Radius dependent BLACK HOLE.

$$\bar{E} = K\, e^{-\frac{G1\varepsilon 0\mu 0}{8\pi r}} \begin{pmatrix} 0 \\ \text{Sin[k r] Sin[}\omega\text{ t]} \\ \text{- Cos[k r] Cos[}\omega\text{ t]} \end{pmatrix} \tag{24}$$

$$\bar{H} = K\, e^{-\frac{G1\grave{o}0\mu 0}{8\pi r}} \sqrt{\frac{\varepsilon_0}{\mu_0}} \begin{pmatrix} 0 \\ \text{Sin[k r] Cos[}\omega\text{ t]} \\ \text{- Cos[k r] Sin[}\omega\text{ t]} \end{pmatrix}$$

Equation (20) represents by the function Sin[k r] (k = 1,2,3,4....) the confinement of electromagnetic radiation between two concentric spheres. K represents the amplitude of the Electric/ Magnetic Field Intensty. [14]

Time and Polar Angle Dependent Black Holes:

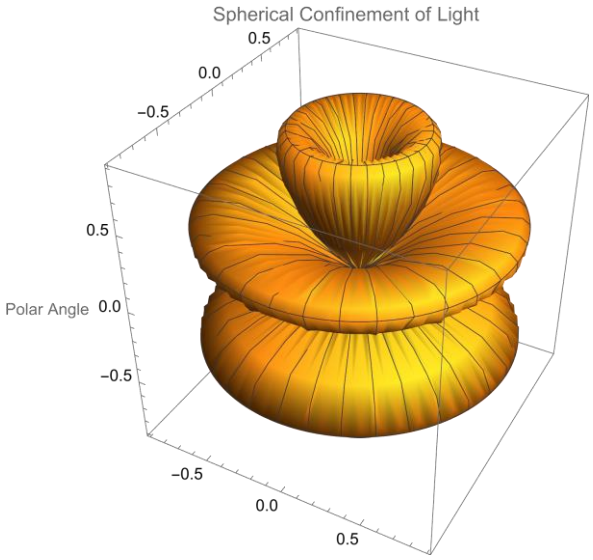

Fig. 7: Nodal- and Antinodal Polar Angle Regions (m = 3) for Standing (Confined) Spherical Electromagnetic waves with a 90 degrees phase shift between the Electric field and the Magnetic field. Equation (15)

Equation (25) describes a Time and "Polar Angle" dependent BLACK HOLE

$$\overline{E} = K\, e^{-\frac{G1\varepsilon 0\mu 0}{8\pi r}} \begin{pmatrix} 0 \\ \text{Sin}[m\ \theta]\ \text{Sin}[\omega\ t] \\ \text{Sin}[m\ \theta]\ \text{Cos}[\omega\ t] \end{pmatrix} \tag{25}$$

$$\overline{H} = K\, e^{-\frac{G1\grave{o}0\mu 0}{8\pi r}} \sqrt{\frac{\varepsilon_0}{\mu_0}} \begin{pmatrix} 0 \\ \text{Sin}[m\ \theta]\ \text{Cos}[\omega\ t] \\ -\text{Sin}[m\ \theta]\ \text{Sin}[\omega\ t] \end{pmatrix}$$

Equation (19) represents by the function $\text{Sin}[m\,\theta]$ (m = 1,2,3,4.....) the confinement of electromagnetic radiation between two Polar Angular Regions [15].

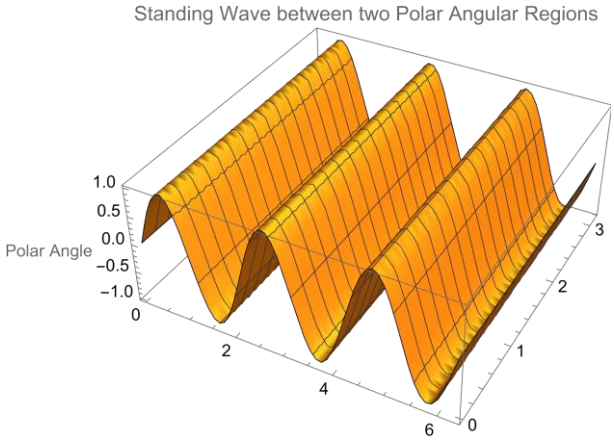

Fig. 8: Nodal- and Antinodal Polar Angle Regions (m = 3) for Standing (Confined) Electromagnetic waves with a 90 degrees phase shift between the Electric field and the Magnetic field. Equation (15)

Time and Azimuthal Angular Dependent Black Holes:

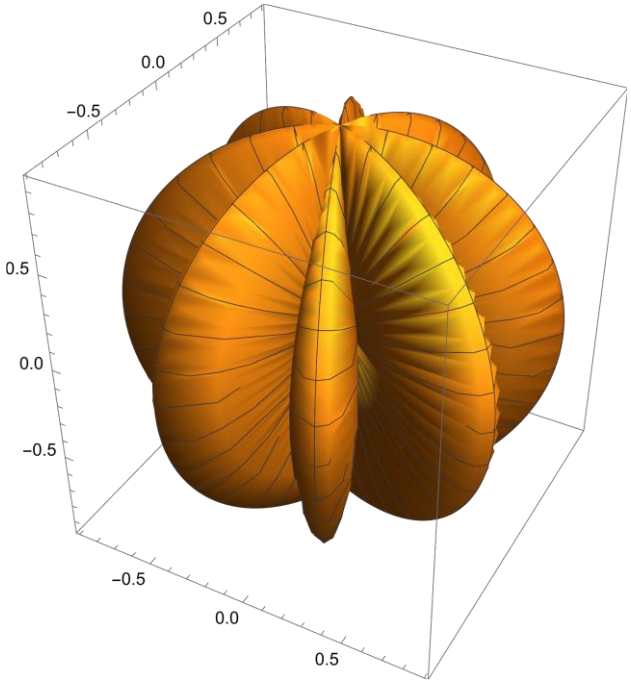

Fig. 9: Nodal- and Antinodal Azimuthal Angular Regions (n = 3) for Standing (Confined) Electromagnetic waves with a 90 degrees phase shift between the Electric field and the Magnetic field. Equation (16)

Equation (26) describes a Time and "Polar Angle" dependent BLACK HOLE

$$\overline{E} = K\, e^{-\frac{G1\varepsilon 0\mu 0}{8\pi r}} \begin{pmatrix} 0 \\ \text{Cos}[n\ \varphi]\ \text{Sin}[\omega\ t] \\ \text{Cos}[n\ \varphi]\ \text{Cos}[\omega\ t] \end{pmatrix} \qquad (26)$$

$$\overline{H} = K\, e^{-\frac{G1\grave{o}0\mu 0}{8\pi r}} \sqrt{\frac{\varepsilon_0}{\mu_0}} \begin{pmatrix} 0 \\ \text{Cos}[n\ \varphi]\ \text{Cos}[\omega\ t] \\ -\text{Cos}[n\ \varphi]\ \text{Sin}[\omega\ t] \end{pmatrix}$$

Equation (26) represents by the function $\text{Sin}[n\ \varphi]$ (n = 1,2,3,4.....) the confinement of electromagnetic radiation between two Azimuthal Angular Regions [16].

Time, Polar- and Azimuthal Angular Dependent Black Holes:

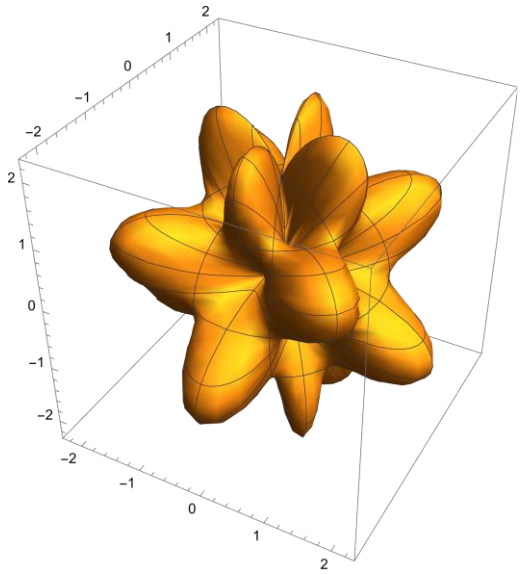

Fig. 10: Nodal- and Antinodal Polar Angular and Azimuthal Angular Regions (n = 4 and m = 4) for Standing (Confined) Electromagnetic waves with a 90 degrees phase shift between the Electric field and the Magnetic field. Equation (17)

Equation (27) describes a Time "Azimuthal Angle" and "Polar Angle" dependent BLACK HOLE

$$\overline{E} = K\, e^{-\frac{G1\varepsilon 0\mu 0}{8\pi r}} \begin{pmatrix} 0 \\ \text{Cos[n } \varphi\text{] Sin[m } \theta\text{] Sin[}\omega\text{ t]} \\ \text{Cos[n } \varphi\text{] Sin[m } \theta\text{] Cos[}\omega\text{ t]} \end{pmatrix} \tag{27}$$

$$\overline{H} = K\, e^{-\frac{G1\eth 0\mu 0}{8\pi r}} \sqrt{\frac{\varepsilon_0}{\mu_0}} \begin{pmatrix} 0 \\ \text{- Cos[n } \varphi\text{] Sin[m } \theta\text{] Cos[}\omega\text{ t]} \\ \text{Cos[n } \varphi\text{] Sin[m } \theta\text{] Sin[}\omega\text{ t]} \end{pmatrix}$$

Equation (27) represents by the function $\text{Cos[n } \varphi\text{]}$ (n = 1,2,3,4…..) and $\text{Sin[m } \theta\text{]}$ (m = 1,2,3,4…..) the confinement of electromagnetic radiation between two Azimuthal Angular Regions and two Polar Angulars Regions [17].

Spherical Confinement of Light Beween Two Concentric Spheres Within Black Holess:

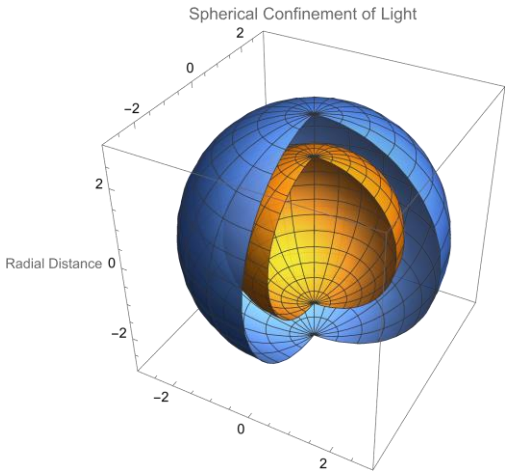

Fig.11: Nodal- and Antinodal Regions for Standing (Confined) Electromagnetic waves with a 90 degrees phase shift between the Electric field and the Magnetic field. Equation (14)

Equation (18) represents the reflection of the Confined Electromagnetic Energy within the BLACK HOLE between two concentric spheres while the speed of light, depending on the variable "r", changes in direction with the frequency of the confined light (Electromagnetic Radiation).

A BLACK HOLE can split into two new BLACK HOLEs with different radi. The original BLACK HOLE falls back into a lower energy level while the new BLACK HOLE represents the difference in Energy Levels comparable with an atom falling back into a lower energy level.

$$\bar{E} = K\, e^{-\frac{G1\varepsilon 0\mu 0}{8\pi r}} f\left[t - \frac{\sqrt{\varepsilon_0\ \mu_0}\ \text{Cos}[2\,k\,r]}{2\,k}\right] \begin{pmatrix} 0 \\ \text{Sin}[k\,r]\ \text{Sin}[\omega\,t] \\ -\text{Cos}[k\,r]\ \text{Cos}[\omega\,t] \end{pmatrix} \tag{28}$$

$$\bar{H} = K\, e^{-\frac{G1\eth 0\mu 0}{8\pi r}} f\left[t - \frac{\sqrt{\varepsilon_0\ \mu_0}\ \text{Cos}[2\,k\,r]}{2\,k}\right] \sqrt{\frac{\varepsilon_0}{\mu_0}} \begin{pmatrix} 0 \\ -\text{Sin}[k\,r]\ \text{Cos}[\omega\,t] \\ -\text{Cos}[k\,r]\ \ \text{Sin}[\omega\,t] \end{pmatrix}$$

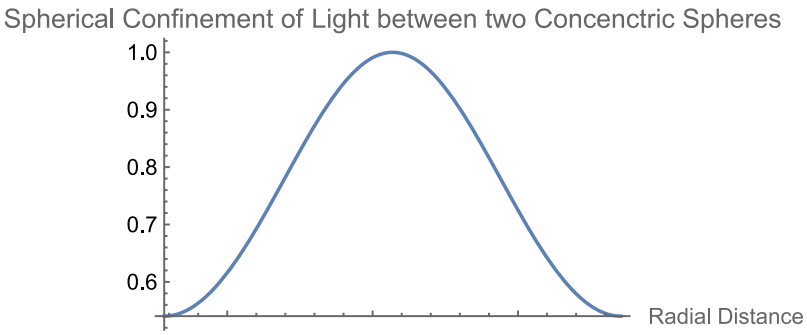

Fig. 12: Nodal- and Antinodal Regions for Standing (Confined) Electromagnetic within two concentric spheres. Equation (18)

UNIVERSAL EQUILIBRIUM IN THE "CONCEPT OF QUANTUM MECHANICAL PROBABILITY" IN "THE NEW THEORY"

The 4-dimensional notation for the divergence of the Stress-Energy Tensor (25) expresses in the 4th dimension (time dimension) the law of Conservation of Energy". For an Electromagnetic Field the law for conservation of Energy has been expressed as:

$$\bar{f}^4 = \begin{pmatrix} f_4 \\ f_3 \\ f_2 \\ f_1 \end{pmatrix} = \square\ \square\, \bar{\bar{T}} = \begin{pmatrix} \nabla \cdot \bar{S} + \frac{\partial\, w}{\partial\, t} \\ f_3 \\ f_2 \\ f_1 \end{pmatrix} = \bar{0}^4 \tag{29}$$

From the equation for the "Conservation of Electromagnetic Energy" (38.1) the "Fundamental Equation for Confined Electromagnetic Interaction" in "The New Theory" will be derived, which equals the Relativistic Quantum Mechanical "Dirac" equation and the Schrödinger wave equation at velocities relatively low compared to the speed of light.

The "Fundamental Equation for Confined Electromagnetic Interaction" in "The Proposed Theory" can be considered to be the relativistic version of the Quantum Mechanical Schrödinger wave equation, which equals the Quantum Mechanical Dirac Equation.

Confined Electromagnetic Energy Within a 4-Dimensional Equilibrium

The physical concept of quantum mechanical probability waves has been created during the famous 1927 5th Solvay Conference. During that period there were several circumstances which came just together and made it possible to create a unique idea of "Material Waves" (Solutions of Schödinger's wave equation) being complex (partly real and partly imaginary) and describing the probability of the appearance of a physical object (elementary particle) generally indicated as "Quantum Mechanical Probability Waves".

The idea of complex (probability) waves is directly related to the concept of confined (standing) waves. Characteristic for any standing acoustical wave is the fact that the Velocity and the Pressure (Electric Field and Magnetic Field in QLT) are always shifted over 90 degrees. The same principle does exist for the standing (confined) electromagnetic waves,

For that reason every confined (standing) Electromagnetic wave can be described by a complex sum vector $\bar{\phi}$ of the Electric Field Vector $\bar{\mathrm{E}}$ and the Magnetic Field Vector $\overline{\mathbf{B}}$ ($\bar{\mathrm{E}}$ has 90 degrees phase shift compared to $\overline{\mathbf{B}}$).

The vector functions $\bar{\phi}$ and the complex conjugated vector function $\bar{\phi}^*$ will be written as:

$$\bar{\phi} = \frac{1}{\sqrt{2\,\mu}} \left(\bar{\mathrm{B}} + \mathrm{i}\, \frac{\bar{\mathrm{E}}}{c} \right) \tag{30}$$

$\overline{\mathbf{B}}$ equals the magnetic induction, $\overline{\mathbf{E}}$ the electric field intensity ($\bar{\mathrm{E}}$ has + 90 degrees phase shift compared to $\overline{\mathbf{B}}$) and c the speed of light.

The complex conjugated vector function $\overline{\phi^*}$ equals:

$$\overline{\phi^*} = \frac{1}{\sqrt{2\,\mu}} \left(\bar{\mathrm{B}} - \mathrm{i}\, \frac{\bar{\mathrm{E}}}{c} \right) \tag{31}$$

The dot product equals the electromagnetic energy density w:

$$\bar{\phi} \,.\, \overline{\phi^*} = \frac{1}{2\,\mu} \left(\bar{\mathrm{B}} + \mathrm{i}\, \frac{\bar{\mathrm{E}}}{c} \right) . \left(\bar{\mathrm{B}} - \mathrm{i}\, \frac{\bar{\mathrm{E}}}{c} \right) = \frac{1}{2}\,\mu\,\mathrm{H}^2 + \frac{1}{2}\,\varepsilon\,\mathrm{E}^2 = \mathrm{w} \tag{32}$$

Using Einstein's equation W = m c², the dot product equals the electromagnetic mass density w:

$$\bar{\phi} \,.\, \overline{\phi^*} \frac{1}{\mathrm{c}^2} = \frac{\varepsilon}{2} \left(\bar{\mathrm{B}} + \mathrm{i}\, \frac{\bar{\mathrm{E}}}{c} \right) . \left(\bar{\mathrm{B}} - \mathrm{i}\, \frac{\bar{\mathrm{E}}}{c} \right) = \frac{1}{2}\,\varepsilon\,\mu^2\mathrm{H}^2 + \frac{1}{2}\,\varepsilon^2\mathrm{E}^2 = \rho\ [\mathrm{kg/m^3}] \tag{33}$$

The cross product is proportional to the Poynting vector (Ref. 3, page 202, equation 15).

$$\bar{\phi} \times \bar{\phi}^* = \frac{1}{2\mu}\left(\bar{B} + i\frac{\bar{E}}{c}\right) \times \left(\bar{B} - i\frac{\bar{E}}{c}\right) = i\sqrt{\varepsilon\mu}\ \bar{E} \times \bar{H} = i\sqrt{\varepsilon\mu}\ \bar{S} \tag{34}$$

This article presents a new "Gravitational-Electromagnetic Equation" describing Electromagnetic Field Configurations which are simultaneously the Mathematical Solutions for the Scalar Quantum Mechanical "Schrodinger Wave Equation" and more exactly the Mathematical Solutions for the Tensor representation of the "Relativistic Quantum Mechanical Dirac Equation" (41).

The 4-dimensional divergence of the sum of the Electromagnetic Stress-Energy tensor expresses the 4-dimensional Force-Density vector (expressed in [N/m³] in the 3 spatial coordinates) as the result of Electro-Magnetic-Gravitational interaction.

$$f^{\mu} = \partial_{\nu} T^{\mu\nu} = 0 \tag{35}$$

In vector notation the 4-dimensional Force-Density vector can be written as:

$$\bar{f}^4 = \begin{pmatrix} f_4 \\ f_3 \\ f_2 \\ f_1 \end{pmatrix} = \square\ \square\ \bar{\bar{T}} = 0 \tag{36}$$

The fundamental boundary condition for this alternative approach to gravity is the requirement that the Force 4 vector equals zero in the 4 dimensions, expressing a universal 4-dimensional equilibrium: The 3 spatial components of the Force-Density vector, as a result of Electro-Magnetic-Gravitational interaction can be written as: Substituting the electromagnetic values for the electric field intensity "E" and the magnetic field intensity "H" in (36) results in the 4-dimensional representation of the Electro-Magnetic-Gravitational Fields Equation (37):

Energy-Time Domain

$$\left(f_4\right) \Leftrightarrow \nabla \cdot \left(\bar{E} \times \bar{H}\right) + \frac{1}{2}\frac{\partial\left(\varepsilon_0\left(\bar{E} \cdot \bar{E}\right) + \mu_0\left(\bar{H} \cdot \bar{H}\right)\right)}{\partial t} = 0$$

(37)

3-Dimensional Space Domain

$$\begin{pmatrix} f_3 \\ f_2 \\ f_1 \end{pmatrix} \Leftrightarrow -\frac{1}{c^2}\frac{\partial\left(\bar{E} \times \bar{H}\right)}{\partial t} + \varepsilon_0\,\bar{E}\,(\nabla \cdot \bar{E}) - \varepsilon_0\,\bar{E} \times (\nabla \times \bar{E})$$

$$+ \mu_0\,\bar{H}\,(\nabla \cdot \bar{H}) - \mu_0\,\bar{H} \times (\nabla \times \bar{H}) = \bar{0}$$

In which f_1, f_2, f_3, represent the force densities in the 3 spatial dimensions and f_4 represent the force density (energy flow) in the time dimension (4^{th} dimension). Equation (37) can be written as:

Energy-Time Domain

Conservation of Energy

B-7

$$\left(f_4\right) \qquad \nabla \cdot \bar{S} + \frac{\partial w}{\partial t} = 0 \qquad (38.1)$$

(38)

3-Dimensional Space Domain

B-1 B-2 B-3

$$\begin{pmatrix} f_3 \\ f_2 \\ f_1 \end{pmatrix} \quad -\frac{1}{c^2}\frac{\partial (\bar{E} \times \bar{H})}{\partial t} + \varepsilon_0 \bar{E}\,(\nabla \cdot \bar{E}) - \varepsilon_0 \bar{E} \times (\nabla \times \bar{E}) +$$

B-4 B-5

$$+\mu_0 \bar{H}\,(\nabla \cdot \bar{H}) - \mu_0 \bar{H} \times (\nabla \times \bar{H}) = \bar{0} \qquad (38.2)$$

The 4^{th} term in equation (38.1) can be written in the terms of the Poynting vector "S" and the energy density "w" representing the electromagnetic law for the conservation of energy (Newton's second law of motion).

The 4-dimensional Relativistic Dirac Equation

Substituting (32) and (34) in Equation (38.1) results in the 4-Dimensional Tensor presentation for the relativistic quantum mechanical Dirac Equation (39):

$$\left(x_4\right) \qquad \nabla \cdot (\bar{\phi} \times \bar{\phi^*}) + \frac{i}{c}\frac{\partial \bar{\phi} \cdot \bar{\phi}^*}{\partial t} = 0 \qquad (39)$$

$$\begin{pmatrix} x_3 \\ x_2 \\ x_1 \end{pmatrix} \quad \frac{i}{c}\frac{\partial (\bar{\phi} \times \bar{\phi^*})}{\partial t} - \left(\bar{\phi} \times (\nabla \times \bar{\phi^*}) + \bar{\phi^*} \times (\nabla \times \bar{\phi}) \right) + \left(\bar{\phi}\,(\nabla \cdot \bar{\phi^*}) + \bar{\phi^*}\,(\nabla \cdot \bar{\phi}) \right) = 0$$

To transform the electromagnetic vector wave function $\bar{\phi}$ into a scalar (spinor or one-dimensional matrix representation), the Pauli spin matrices σ and the following matrices (Ref. 3 page 213, equation 99) are introduced:

$$\bar{\alpha} = \begin{bmatrix} 0 & \sigma \\ \sigma & 0 \end{bmatrix} \quad \text{and} \quad \bar{\beta} = \begin{bmatrix} \delta_{ab} & 0 \\ 0 & -\delta_{ab} \end{bmatrix} \qquad (40)$$

The Equations (6), (32) and (34) can be written in tensor presentation as the 4-Dimensional Relativistic Quantum Mechanical Dirac Equation: [3] (Equation 102, page 213)

$$\left(x_4\right) \qquad \left(\frac{i\,m\,c}{h}\,\bar{\beta} + \bar{\alpha}\,.\,\nabla\right)\psi = -\frac{1}{c}\,\frac{\partial\psi}{\partial t} \qquad (41.1)$$

(41)

$$\begin{pmatrix} x_3 \\ x_2 \\ x_1 \end{pmatrix} \quad -\frac{1}{c^2}\frac{\partial\,(\bar{E}\times\bar{H})}{\partial t} + \varepsilon_0\,\bar{E}\,(\nabla\,.\,\bar{E}) - \varepsilon_0\,\bar{E}\times(\nabla\times\bar{E}) + \qquad (41.2)$$

$$+\,\mu_0\,\bar{H}\,(\nabla\,.\,\bar{H}) - \mu_0\,\bar{H}\times(\nabla\times\bar{H}) + \gamma_0\,\bar{g}\,(\nabla\,.\,\bar{g}) - \gamma_0\,\bar{g}\times(\nabla\times\bar{g}) = \bar{0}$$

CONCLUSIONS

Based on the assumption of the zero-rest mass of photons, General Relativity describes the interaction between Gravity and Light within a 4-dimensional curvature in Space and Time due to a gravitational field. Light follows a path defined y this curved 4-dimensional Space and Time geometry.

The new theory, describes a bi-directional separation between mass and inertia for light (photons). Inertia can only exist only in the direction of propagation of the beam of light (photons) which determines the speed of light. Mass of the beam of light (photons) can only exist in the plane perpendicular to the direction of propagation (directions of confinement), which determines the deflection of a beam of light (photons) by a gravitational field in the plane perpendicular to the direction of propagation.

BLACK HOLEs (Gravitational-Electromagnetic Confinements) are fundamental solutions of the relativistic quantum mechanical Dirac equation. Black Holes represent the large impact of "Gravitational Intensity Shift" and "Gravitational RedShift" due to a gravitational field. Both phenomena can maybe observe in the future with extremely sensitive observatories at extreme low frequency levels.

The new theory describes the impact of "CURL" [38] within the gravitational fields around Black Holes and the impact on Gravitational Lensing. Gravitational "CURL" (Equation 6) is an effect which cannot be explained and calculated by General Relativity

Within a 4-Dimensional Equilibrium and taking into account the inertia- and the gravitational-force densities within the electromagnetic field configurations, Gravitational Electromagnetic Confinements (BLACK HOLEs at sub-atomic dimensions) are a physical reality and are solutions of the Relativistic Quantum Mechanical Dirac Equation (39, 41) and present spherical confinements with discrete separate energy levels.

To test the proposed theory with General Relativity, an experiment [2] has been required which measures the interaction between gravity and light within a well-defined gravitational field like the gravitational field of the earth. The difference between the calculation for Gravitational RedShift, within the Gravitational Field of the Earth, in "General Relativity" and "The New Theory" is smaller than 10^{-16} and cannot be determined with present observation equipment (maximum accuracy of 10^{-15} for GRS). Validation of both theories requires higher accuracies.

Dark Matter does exist because of "Gravitational RedShift" and Gravitational Intensity Shift". A complete Galaxy, existing of billions bright light emitting star constellations, with a total mass of

10^{53} [kg] becomes invisible for any observatory like the "James Webb Space Telescope" at the distance of 5 10^{21} [m] (which is 10 times the radius of the Milky Way Galaxy). This distance of "Gravitational Shielding" has been controlled by the mathematical solution (20) for equation (8). The gravitatonal field of these Galaxies has not been effected by the effect of "Gravitationa RedShift" and "Gravitational IntensityShift" at all.

For this reason a large percentage of the total mass in the Universe beyond te border of "Gravitational Shielding" becomes invisible for our observatories on and close around the earth. While the gravitational fields of these galaxies still has the full influence on our universe.

Nuclear fusion represents the border area (nuclear plasma) between the material world (infusion of Deuterium) and the energy world (microwave heating). Existing theories to describe these material-energy interactions are far from the required necessary theoretical physics to realize stable nuclear fusion processes inside confinements like the Tokamak. The only possibility to describe these complex "mechanical-electromagnetic" interaction processes correctly is to develop a new theory in physics which describes the electro-magnetic-gravitational (linear- or rotational acceleration) force density interactions (expressed in N/m^3) (equation 8) with the mechanical force density interactions (expressed in N/m^3) being presented by the Navier-Stokes equation for compressible nuclear plasmas [41].

Equation (42) and for laminar Plasma Flows (45) represents te 3-dimensional equilibrium between all the dynamic- and electromagnetic force densities within the nuclear plasma and comsequently the fundamental stability requirements for nuclear fusion.

Data Availability

All Data and Calculations have been published at: https://quantumlight.science/

REFERENCES

[1] Wheeler; John Archibald; GEONs, Physical Review Journals Archive, 97, 511, Issue 2, pages 511-526, Published 15 January 1955, Publisher: American Physical Scociety, DOI: 10.1103/PhysRev.97.511:

[2] Sven Herrmann, Felix Finke, Martin Lülf, Olga (et. Al.) l; Test of the Gravitational Redshift with Galileo Satellites in an Eccentric Orbit; Phys. Rev. Lett. **121**, 231102 – Published 4 December 2018; Gravitational Redshift Test Using Eccentric Galileo Satellites, DOI: 10.1103/PhysRevLett.121.231102

[3] Vegt, J. W. A Continuous Model of Matter based on AEONs, Physics Essays, Volume 8, Number 2, 1995, DOI: 10.31219/osf.io/ra7ng

[4] Mathematical Solutions for the Propagation of Light in Quantum Light Theory, Calculations in Mathematica 13.1: https://community.wolfram.com/groups/-/m/t/2576692?p_p_auth=mTldHX3v

[5] Gravitational RedShift between two Atomic Clocks, Calculations in Mathematica 13.1: https://community.wolfram.com/groups/-/m/t/2622560?p_p_auth=EC8QO0Xz

[6] Propagation of Light within a Gravitational Field in Quantum Light Theory, Calculation in Mathematica 13.1: https://community.wolfram.com/groups/-/m/t/2576537?p_p_auth=iljE3giH

[7] Raymond J. Beach; A classical Field Theory of Gravity and Electromagnetism; Journal of Modern Physics; 2014, 5, 928-939

[8] Maxwell; James Clerk; A dynamical theory of the electromagnetic field; 01 January 1865; https://royalsocietypublishing.org/doi/10.1098/rstl.1865.0008

[9] A. Einstein; On the Influence of Gravitation on the Propagation of Light; Annalen der Physik (ser. 4), 35, 898–908, http://myweb.rz.uni-augsburg.de/~eckern/adp/history/einstein-papers/1911_35_898-908.pdf

[10] Mahendra Goray, Ramesh Naidu Annavarapu, Rest mass of photon on the surface of matter, Results in Physics 16 (202) 102866, January 2020, DOI: 10.1016/j.rinp.2019.102866

[11] Genova, A., Mazarico, E., Goossens, S. et al.; Solar system expansion and strong equivalence principle as seen by the NASA MESSENGER mission; Nat Commun 9; 289 (2018). DOI: 10.1038/s41467-017-02558-1

[12] John G. Williamson; A new linear theory of light and matter; 2019; J. Phys.: Conf. Ser. 1251 012050 DOI 10.1088/1742-6596/1251/1/012050

[13] BLACK HOLEs with Discrete Spherical Energy Levels: https://community.wolfram.com/groups/-/m/t/2896941?p_p_auth=D7ZKu03k

[14] Time and Radius dependent GEONs with discrete Energy Levels. https://community.wolfram.com/groups/-/m/t/2900869?p_p_auth=yxR9nZu6

[15] Time and Angular Regions dependent GEONs with discrete energy levels. https://community.wolfram.com/groups/-/m/t/2901457?p_p_auth=H4jjDHmQ

[16] Time and Azimuthal Regions dependent GEONs with discrete energy levelshttps://community.wolfram.com/groups/-/m/t/2902170?p_p_auth=ytoq5nEh

[17] Time, Polar Angular and Azimuthal Angular Regions dependent GEONs with discrete energy levels https://community.wolfram.com/groups/-/m/t/2902642?p_p_auth=sW2mvv9L

[18] D. W. Sciama; The Physical Structure of General Relativity; Rev. Mod. Phys. 36, 463 – Published 1 January 1964; Erratum Rev. Mod. Phys. 36, 1103 (1964)

[19] Adrian del Rio, Jose Navarro-Salas, and Francisco Torrenti; Renormalized stress-energy tensor for spin -1/2 fields in expanding universes; Phys. Rev. D 90, 084017 – Published 13 October 2014

[20] Stergios Pellis; Unity Formulas for the Coupling Constants and the Dimensionless Physical Constants; Journal of High Energy Physics Gravitation and Cosmology; DOI: 10.4236/jhepgc.2023.91021

[21] Bloch, Yakov and Joshua Foo. "How the result of a measurement of a photon's mass can turn out to be 100." (2023). Corpus ID: 258426255

[22] Andrés Arámburo García, Kyrylo Bondarenko, Sylvia Ploeckinger, Josef Pradler and Anastasia Sokolenko; Effective photon mass and (dark) photon conversion in the inhomogeneous Universe; Journal of Cosmology and Astroparticle Physics, Volume 2020, October 2020

[23] Alexander M Gabovich and Nadezhda A Gabovich; How to explain the non-zero mass of electromagnetic radiation consisting of zero-mass photons; European Journal of Physics; 2007; 28 649; DOI 10.1088/0143-0807/28/4/004

[24] Liang-Cheng Tu, Jun Luo and George T Gillies; The mass of the photon; Reports on Progress in Physics, Volume 68, Number 1; DOI 10.1088/0034-4885/68/1/R02

[25] Doyon, B. Conformal Loop Ensembles and the Stress–Energy Tensor. Lett Math Phys 103, 233–284 (2013). https://doi.org/10.1007/s11005-012-0594-1

[26] T. P. Hack and V. Moretti; On the stress–energy tensor of quantum fields in curved spacetimes—comparison of different regularization schemes and symmetry of the Hadamard/Seeley–DeWitt coefficients; 2012 J. Phys. A: Math. Theor. 45 374019; DOI: 10.1088/1751-8113/45/37/374019

[27] Adam Levi; Renormalized stress-energy tensor for stationary black holes; Phys. Rev. D 95, 025007 – Published 10 January 2017; https://doi.org/10.1103/PhysRevD.95.025007

[28] Gobbi, Julio; Luminiferous Æther: General Science Journal; December 10, 2018 γ_0 = Gravitational permeability of vacuum [kg s2 m-3]

[29] Xing-Hao Ye, Qiang Lin; Gravitational Lensing Analyzed by Graded Refractive Index of Vacuum; Journal of Optics A: Pure and Applied Optics; 1 May 2008; DOI 10.1088/1464-4258/10/7/075001

[30] Wim Vegt; "The Origin of Gravity in "Quantum Light Theory""; OSF Preprints; October 14. doi:10.31219/osf.io/n43yd

[31] P. Delva, N. Puchades, E. Schönemann, F. Dilssner, C. Courde (et. all); Gravitational Redshift Test Using Eccentric Galileo Satellites; Phys. Rev. Lett. 121, 231101 – Published 4 December 2018; DOI: 10.1103/PhysRevLett.121.231101

[32] Oppenheim, Jonathan, A Postquantum Theory of Classical Gravity, Phys. Rev. X, Vol. 13, December 2023; DOI: https://doi.org/10.1103/PhysRevX.13.041040

[33] Wim Vegt, The Origin of Gravity, A second order Lorentz Transformation for "Accelerated Electromagnetic Fields", Generating a Gravitational Field and the property of Mass, International Research Journal of Pure and Applied Physics Vol.9 No.1, pp.12-52, 2022.

[34] Wim Vegt, The 4-Dimensional Dirac Equation in Relativistic Field Theory, European Journal of Applied Sciences, Vol 9, No. 1, pp 35 – 93,2021

[35] Wim Vegt; A Perfect Equilibrium inside a Black Hole; Wolfram Community: https://community.wolfram.com/groups/-/m/t/3087823?p_p_auth=dpH7iBMg

[36] Albert Einstein, "Elementare Uberlegungen zur Interpretation der Grundlagen der Quanten-Mechanik", Translated into English, 2011, DOI: https://doi.org/10.48550/arXiv.1107.3701

[37] Nikko John Leo S. Lobos, Reggie C. Pantig; Generalized Extended Uncertainty Principle Black Holes: Shadow and lensing in the macro- and microscopic realms; Physics 2022, 4(4), 1318-1330; https://doi.org/10.3390/physics4040084

[38] Zihua Weng, Influence of velocity curl on conservation laws, October 2008, https://doi.org/10.48550/arXiv.0810.0065

[39] Peter Vadasz, Rendering the Navier–Stokes Equations for a Compressible Fluid into the Schrödinger Equation for Quantum Mechanics, MDPI-Fluids, May 2016, https://doi.org/10.3390/fluids1020018

[40] Young-Sam Kwon, Asymptotic limit for rotational quantum compressible Navier–Stokes equations with multiple scales, Journal of Mathematical Analysis and Applications, Volume 464, Issue 2, 15 August 2018, Pages 1408-1424, https://doi.org/10.1016/j.jmaa.2018.04.073

[41] Senjo Shimizu and Hidenobu Tsuritani, on a Navier–Stokes–Ohm problem from plasma physics in multi connected domains, Partial Differential Equations and Applications (2021) 2:75, https://doi.org/10.1007/s42985-021-00122-7

[42] Jean-Luc Cambier and David A. Micheletti, Theoretical Analysis of the Electron Spiral Toroid Concept, NASA/CR-2000-210654, https://ntrs.nasa.gov/api/citations/20010021117/downloads/20010021117.pdf

[43] Soraya Field Fiorio, Isaac Newton: Magician, https://parabola.org/2020/11/01/isaac-newton-magician/

[44] Egil Asprem, The problem of disenchantment: scientific naturalism and esoteric discourse, Amsterdam University,1939

[45] The Emerald Tablet of Hermes & The Kybalion; ISBN-13: 9781911405269

[46] J.D. Sethian, M. Friedman e.a.; Fusion energy with lasers, direct drive targets, and dry wall chambers; Nuclear Fusion, Volume 43, Number 12; **DOI** 10.1088/0029-5515/43/12/015

Applied Sciences Research Periodicals – ISSN 3033-330X
March 2024, Vol. 2, No. 3, pp. 51-60

When the Holiday Goes South: Case Study of Norovirus Outbreak and Overview of Common Food and Water Borne Illnesses

Vorachoat Karunyasopon[4] George P Einstein[1,2], Frantz Sainvil[1-3], Syed A. A. Rizvi[5], and Orien L Tulp[1,2]

1. Colleges of Medicine and Graduate Studies, University of Science Arts and Technology, Montserrat BWI
2. Einstein Medical Institute, NPB, FL USA
3. Broward University, FL USA
4. National University of Medical Sciences, Spain
5. Larkin Hospital, Miami FL USA

Abstract:
A recent outbreak of norovirus occurred approximately 24 hours into a cruise, while passengers were enroute to a Northern destination aboard a holiday cruise ship on a scheduled week-long journey. The symptoms of classic norovirus including watery diarrhea, severe abdominal cramps and nausea were quickly recognized, and the illness causation confirmed via on-board laboratory testing in the ship infirmary. Appropriate treatment prescribed by the ship's physician, and containment was realized within a few days. Because of the limited number of passengers affected (12 out of over 1,000), and the timing of the incident, it was concluded that the origin of the infection likely occurred prior to or soon after the passengers boarded, possibly linked to a welcoming ceremony hosted by the ship's captain during which a variety of h'odoerve style finger foods including some seafood items were made available during a buffet dinner. Following the initial outbreak, no additional cases were reported or identified, no on-board origin was confirmed, and all passengers recovered without incident and continued the cruise.

Keywords: Norovirus, Food borne illness, episode, cruise ship, outbreak.

INTRODUCTION

Foodborne and waterborne illness (FWBI) represent an ever-present potential risk at home and abroad and present a significant cause of morbidity and mortality in the United States and other countries. 1,2 FWBI can be caused by numerous entities, including heavy metals, toxins of biological or other origin, bacteria, viruses, and parasites. 3 According to the CDC, approximately 48 million people become ill from foodborne and waterborne diseases each year, stemming from 10 or more commonly reoccurring noxious or pathophysiologic agents. The most common vector is unintentional consumption of contaminated food, water, or beverages that have been consumed and thus introduced into the food chain of the unsuspecting host or hosts via the fecal-oral route of transmission. Of the 48 million or more cases annually, approximately 128,000 require hospitalization, and unfortunately, some 3,000 or more may succumb to a food or waterborne illness in any given year. 1-4 Food safety is a major concern in most Westernized nations, where the food processing systems and retail providers often typically employ an unparalleled level of scrutiny during manufacture, testing, storage and final table presentation, but when breeches in the system occur, the unintended consequences may be substantial.

Despite the precautions, as many one in 6 restaurant diners may experience a food borne related illness in any given year according to the CDC reports. 3-5.

Contributing to this high incidence are factors that may occur as the consumable items become contaminated at any stage of the origination or intermediate processes leading up to the serving of the dining clientele. 4 Because potential sources such as uneaten left-over food items are often discarded and thus no longer available for survey by the time symptoms are first reported, positive confirmation of the origin may not always be readily attainable. In addition, some patients and experienced travelers experiencing less severe symptoms may self-medicate unreported episodes without reporting to the infirmary for confirmation or documentation of their illness. Accordingly, it sometimes poses difficulty in determining where or at what stage of food production the contamination may have occurred, and what specific steps must be taken to contain the impending illnesses as was the situation in this outbreak. A brief overview of some common causes of FWBI is summarized below.

Typical common causes of FWBI include viral, microbial, parasitic, and chemical agents. 1,3 These include such items as Listeria monocytogenes, a microbial contamination often found in cantaloupe fruit that may have been surface contaminated from natural fertilizers including manure, and inadequately cleansed and decontaminated melons prior to cutting and serving. 6-8 Over 8,000 reports of 138,000 cases of listeriosis were reported from 2011 to 2020, nearly 10,000 hospitalizations, and 241 deaths. As with many types of infectious illness, those individuals who are in their later years, and those with compromised immunity and other comorbidities and infants typically present the greatest risk of morbidity and mortality from the consequences of FWBIs. Globally, over a billion individuals may be infected with a parasitic illness of one kind or another at any given time, often by way of compromises in industrial hygiene and contaminated foods, beverages, and public water sources. 2,3,9.

Of common parasitic illnesses, helminthic tapeworms reign among the supreme. 3,8,9 The beef/pork tapeworms Taenia saginata (beef origin), Taenia solium (pork origin) and Taenia asiatica (Asian tapeworm) are classed as cestodes, causing mostly intestinal illness with significant gastrointestinal distress, while Taenia solium can also cause cysticercosis. In addition, prolonged duration of cestodal infection may also be marked with nutritional deficiencies, as the rapidly developing parasites consume vitamin B12 and other essential nutrients during their life cycle, thereby preventing their intestinal absorption by their unsuspecting host. The protozoal agent Giardia Lamblia is often found in contaminated, unprotected and untreated water sources including rivers, streams and unprotected springs due to human and animal contamination, and also causes typical gastroenteritis illness. 9,10 While both intestinal cestodes and protozoal infestations are readily treated with antiparasitic agents, care must be taken to ensure clothing and linens are adequately cleansed and decontaminated to prevent re-exposure that could predispose to fecal-oral reinfection. In addition, infection with cryptosporidium species organisms (due to C. hominis or C. parvum) ranks among the most common recreational waterborne parasitic infections to occur in the United States, and also occurs via consumption or exposure to water sources including public pools that have become contaminated. 11,12 The parasite causes gastroenteritis and watery diarrhea that that may persist for up to two weeks following infection, and often fails to fully resolve in the absence of definitive pharmacotherapy. The parasite is relatively resistant to common water chlorination as is commonly applied in private or public pools as a disinfection agent with proven effectiveness for many other potential contaminating organisms. Symptoms of acute diarrhea and enteritis typically commence about

a week after exposure to infective oocytes of cryptosporidia species if consumed via ingestion of the polluted water or by person-to-person direct contact via the fecal-oral route. 9 Entamoeba histolytica is another infectious parasite that can cause amoebiasis followed by severe intestinal inflammation. 9,13,14 It is an anaerobic parasitic amoebozoan organism that can survive outside the body for a considerable time, and can infect humans and other primates including canines. Because Entamoeba histolytica can survive outside the body for a time, it can be readily transmitted by the fecal-oral ingestion route from contaminated food or fingers. Amoebiasis has been estimated to infect about 35-50 million people worldwide, resulting in approximately 55,000 deaths annually due to the severity of the pathobiologic consequences of the organism. The trophozoite form of the parasite can migrate from infected intestinal tissues where it multiplies and can travel via the circulatory system to infect other tissues distant from its origin including lungs, brain, and liver. 9,13,14. Bacillus cereus species are yet another occasional culprit in the area of food-borne illnesses. 9,15 These bacteria are Gram-positive rod-shaped, spore-forming microbes that may be commonly found in soil, food, and marine sponges, and because they are capable of forming persistent biofilms on glass surfaces, they may pose complications of contamination risk during pharmaceutical manufacturing processes. The spores are easily spread via airborne droplets and can also cause moderate, typically non-life-threatening gastrointestinal infection when present in improperly stored or left-over foods. The bacterium readily utilizes glucose as its primary energy source, which represents approximately 98% of its metabolizable energy pathways. 9 While ordinary cooking temperatures can kill the bacteria, the spores are typically somewhat hardier, require a longer and higher temperature to inactivate, and often survive lower cooking and warming temperatures and emerge as active bacterial colonies in stored or warmed foods. Their unique contributions to FWBI remain an ongoing threat to pharmaceutical manufacturers, restaurants, and other instances where foods may be left open to airborne spore contamination on warming tables, serving trays, and other suitable environments. 15 The pathogenic 0157:H7 serotype of Escherichia coli also forms a constant threat for FWBI illness in raw or undercooked beef, milk, salads, and other vegetables that may have become inadvertently contaminated by direct or indirect exposure to bovine manure residues during vegetable propagation, or to meat processing. 9 The contamination occurs from storm or water run-off during heavy rains or irrigation processes. This serotype strain produces a Shiga-like toxin that may result in hemorrhagic diarrhea, hematologic uremic syndrome (HUS) in which red blood cells are destroyed, resulting in kidney failure. The most susceptible include young children, the elderly, and immunocompromised adults. The mode of transmission is via the fecal–oral route, and most reported illnesses have occurred via commercial distribution of contaminated raw leaf green vegetables, undercooked ground meat and raw milk. In the US, 2-7 % of children develop HUS, which is the leading cause of acute kidney failure among young children. Children under the age of 5 years are at significant risk for the direst of consequences when exposed to this microbe. 3,9.

Additional causes of gastrointestinal infection of bacterial origin include Shigella (shigellosis), Salmonella (salmonellosis), and Cholera (cholera) and are caused by facultative, anerobic gram negative bacteria that may inhabit the intestinal tract of humans and occasionally a few other primates. 9 Shigellosis species comprises of different 4 strains of the organism that result in varying degrees of illness from a mild traveler's diarrhea to a severe diarrhea. Shigella bacteria appear to be genetically related to enterohemorrhagic E. coli (E. coli 0157:H7) and represent a common cause of diarrheal illness. The organisms produce variable strain-specific syndromes of diarrhea and bacillary dysentery, gastroenteritis, and is typically characterized by abdominal pain and discomfort, bloody diarrhea (< 20 bowel movements/day), nausea, fever, and vomiting.

The onset of symptoms may occur from 12 hours to two weeks following exposure, which may occur with an inoculum of only 10 or more of the most virulent infective bacteria. The most virulent strain (S. dysenteriae) produces an inflammatory Shiga toxin that attaches to M cells in the epithelial lining of the small intestine, where the organism multiplies rapidly, and can cause breaks in rRNA and intestinal lining, and enhance the release of inflammatory cytokines. The inflammatory cytokines can also damage renal epithelium and contribute to hemolytic uremic syndrome. Shigella organisms are notoriously resistant to macrophage inactivation, and usually require antimicrobial and rehydration therapy. The CDC reports that Shigellosis may affect up to 450,000 individuals per year and mortality can be as high as 20% in those most severely affected. Young children and the elderly/immunocompromised are among the most susceptible groups and is easily spread via the fecal-oral route via contaminated foods and fingers. 1-3,9

Salmonellosis is caused by another group of facultative, anaerobic gram-negative bacterial organisms, resulting in strain specific illnesses including gastroenteritis (s. enteritidis; dysentery) and typhoid fever (S. typhi) in the most pathogenic strains. 9 Of the approximately 2,000 serovars of Salmonella organisms, only about 50 are commonly isolated from human feces. They are common asymptomatic inhabitants in poultry and are difficult to control in the commercial poultry industry and thus mandate thorough sanitation measures and cooking temperatures during preparation. That rare celebratory delicacy of 'pheasant under glass" or holiday 'turkey w/gravy' banquet may be just the opportunity your salmonella has been waiting for! The Salmonella organisms infect the intestinal lining of humans, where they can multiply within intestinal epithelial cells and M cells and can enter the circulation via the intestinal vascular/lymphatic network, and travel to many tissues distant from the intestinal tract, including the spleen, liver, and other organs. Once in the circulation, the bacteria may cause bacteremia and septic shock. 1-3,9 Of the 1.4 million cases reported annually in the US, fewer than 1% (~400) prove to be fatal. The organisms may survive asymptomatically in the human intestinal tract in 1 to 3% of previously infected individuals for many months which likely contributes to their persistence among human populations. Classic symptoms of salmonella infection include diarrhea and moderate fever and may require rehydration and antimicrobial therapy to resolve the problem.

Cholera infection commonly follows environmental disasters and can persist for many years following an outbreak. 9,16,17 Cholera outbreaks can occur wherever contaminated water can infiltrate the domestic water and food supply including typical home or commercial usage of unclean water. Cholera is caused by the 0.1 And O:139 strains of Vibrio cholerae, a motile, morphologically curved gram-negative organism. An active infection usually requires a large number of organisms (~100,000) to be consumed as stomach acid can inactivate the organism; of those that survive the gastric environment, the readily multiply in the intestinal tract, where they produce a potent endotoxin capable of causing extraordinary and profound loss of water and electrolytes via vomiting and diarrhea, with especially severe loss of potassium along with sodium within only hours after infection.

The extraordinary loss of water and electrolytes can cause hypovolemic shock and become fatal in up to 50% of previously healthy individuals, but early intervention with both oral and intravenous rehydration can prevent most deaths. Because of the sodium loss, oral rehydration should contain 5% glucose in order to support sodium-glucose cotransport across the luminal epithelium. The recent epidemic of Cholera in Haiti was caused by fecal contamination of a community water supply and persisted for nearly a decade (2010-2019) and resulted in XXXX

infections XXX deaths. 16,17. Unlike most infectious agents, histamine poisoning via contaminated fish is a heat-stable chemically mediated agent and thus is not destroyed by ordinary cooking temperatures. 18 Decomposing fish (most often in decomposing mackerel, grouper, and amberjack species) may enzymatically convert the endogenous amino acid histidine to histamine, resulting in acute sympathetic, histaminergic reactions, and occasional hospitalizations. In addition, Ciguatera fish poisoning, or CFP represents yet another form of chemical fish poisoning. This FWBI agent is found in herbivorous fish found in reef waters. The ciguatoxins are originally made by, Gambierdiscus toxicus, a small marine organism that grows on and around coral reefs in tropical and subtropical waters. The suspect fish flesh becomes contaminated with the ciguatoxins produced via bioconcentration as larger, carnivorous fish dine on the herbivores. The agent causes diarrhea, vomiting, numbness, heat sensitivity to hot and cold, cardiovascular, and other symptoms including hypotension, which may persist for several weeks or longer following recovery from the acute effects. The diagnosis of histamine or ciguatoxin poisoning is typically based on a person's symptoms and recent history of fish consumption. 9,18,19 If a number of individuals consumed the same fish during the same timeframe also develop symptoms, the diagnosis becomes more probable without further testing, but if some of the questionable fish is still available it can be tested to further confirm the presumptive diagnosis of histamine or CFP poisoning. 9,18,19

Aflatoxins, ergot alkaloids, and botulinum poisoning are additional chemical entities that can cause serious illness in man and animals. 8,20-23 Aflatoxins consist of a group of poisonous, mutagenic, mitotoxic and carcinogenic chemicals that are produced by various species of aerobic Aspergillus fungi. The notorious fungi are also sometimes referred to as molds that normally grow in soil and decaying vegetation, and they can easily thrive on virtually any unrefrigerated or inadequately stored foodstuff, including vegetables, grains, nuts, and spices. Of the various chemical forms including AF B 1, B 2, G 1, G 2 M 1, M 2, L, and Q 1, Aflatoxin B 1 is produced by both A. flavus and A. parasiticus strains and is considered the most toxic form to affect humans and animals, where it causes often fatal carcinomas of the liver and other organs. 20,22.

Ergotism is caused by ergot alkaloids, toxic chemicals that are formed by molds that often grow on rye plants and inadvertently become carried over to rye flour during its manufacture. 9,22 When ergots are accidentally consumed in sufficient quantities, they typically cause a variable, dose related range of vasoconstrictions in the CNS and peripheral tissues, causing hallucinations, peripheral vasoconstriction, vascular collapse and often death. The toxic alkaloids may be blended in such that use of the flour in baking bread and other baked goods resulted in ergot toxicity in the baked goods primarily intended for human consumption. The earliest historical reports of what now appears to have been ergot poisoning in rye bread extends back for many centuries, over 1000 years, until the source and composition active principle was ultimately discovered. 8,22-25 Scientific study of the ergot alkaloids eventually gave rise to the development of LSD (lysergic acid diethylamide) by Hofman, and continue to be studied for possible therapeutic benefits for certain psychological and psychiatric disorders including PTSD. 26

Botulinum poisoning represents yet another potential source of severe adverse effects, as the toxin is formed by Clostridium botulinum. 27 C. botulinum is an obligate anaerobic endospore-forming gram-positive bacillus that is commonly found recently tilled soil and aquatic drainage sediments, where the heat stable endospores can become transmitted to food crops nourished by the nutrients found in the soil and aquatic resources. 9 When present in anaerobic environments such as sealed canned goods, the microorganisms release a potent neuroinhibitory

exotoxin that is highly specific for synaptic acetyl choline receptors, thereby blocking the parasympathetic element of neuromuscular transmission.

Toxicity with the exotoxin results in a flaccid paralysis of muscle fibers, which may persist for 1 to 10 days, dependent on the magnitude of the inhibition. 9 The neuromuscular blockade becomes clinical apparent with secondary symptoms such as nausea and generalized weakness within the first day of exposure but left untreated can result in fatal respiratory distress and cardiac failure within a few days of exposure. The pharmacologic effects of botulinum toxin gave way to the pharmaceutical development of Botox, where extremely small doses are injected into specific muscle groups as a cosmetic procedure to control unsightly wrinkles. 27 Clostridium tetani is another strain of Clostridia sp. that presents as an obligate anaerobic endospore- forming gram-positive bacillus that is commonly found recently tilled soil and aquatic drainage sediments. 9,28 C. tetani produces the neurotoxin tetanospasmin, the definitive cause of tetanus, which like botulinum toxin, also affects skeletal muscles, but by blocking muscle relaxation rather than excitatory pathways. Early symptoms produce the condition known as lockjaw, a condition in which the mouth can no longer open, and swallowing is inhibited, followed by spasms of muscles of the back, head, extremities, and heels to bow in a backward position (opisthotonos), and death via spasms of the respiratory muscles. The organism flourishes in anaerobic environments including deep puncture wounds, where it can continue to produce the neurotoxin, and unlike botulinum poisoning, although phylogenetically related, C. tetani does not commonly occur in edible foods and tetanus is easily prevented by vaccination early in life as part of the DPT vaccine followed by periodic boosters for most individuals, thereby preventing most cases nowadays. 9,28.

Commonly occurring viral agents that cause FWBI include both norovirus and rotavirus, RNA viruses that pose significant risks to infants, young children and older adults. 9,29 Norovirus infection is caused by highly transmissible strains of the RNA-norovirus and typically presents as a food borne illness that is responsible for approximately 50% of the FWBI illnesses causing nonbacterial foodborne gastroenteritis that are reported in the United States; norovirus is responsible for over 80% of FWBI episodes that occur on board of International Cruise ships, a staggering incidence! 2,4,5 Norovirus infection typically produces symptoms of nausea, intestinal cramps, diarrhea, malaise, and dehydration ± a low-grade fever within 18-48 hours post exposure to the infectious viral agent.

The diagnosis is readily confirmed via a sensitive, rapid RIA or PCR analysis of stool specimens, which facilitates an early onset of an appropriate treatment regimen. 9 Norovirus infection is considered the most common non-bacterial cause of FWBI infection in the US, where it is linked to approximately 20 million cases annually, with approximately 300 deaths resulting from the infection. 29 Norovirus infection can be transmitted via food, water and aerosol contaminated surfaces, thus accounting for the high incidence of FWBI infections on international cruise ships (95 outbreaks between 2011- 2019). 2 Infection with norovirus causes injury and inflammation to the microvilli lining the small intestine, resulting in the classic symptoms of watery diarrhea, severe cramps, low grade fever, and generalized abdominal distress. Cleanup following an outbreak is challenging due to the aerosol microdroplet nature that contributes to its dissemination. 4,5 Understandably, cruise ships that are bound for international destinations take considerable time to prepare for the intended journey, spend many days away from port while at sea, and must load enormous quantities of food and other edible consumables prior to departure, since while on board dining options are limited to only what the vessel dining services can provide.

On board storage and preparation may not always occur under opportune environmental or working conditions and may be further compromised by the loading schedules and restocking options at ports of call, which may lead to interruptions in refrigeration or optimal transit conditions. Vessels often travel great distances en route, where unforeseen environmental and human conditions that could compromise food storage and preservation may also occur. The overall complexity of the procurement, monitoring and delivery of the dining options poses opportunities for the weakest link in the system to materialize.

In addition to noroviruses summarized above, infants and young children are also susceptible to rotavirus infection, another viral species phylogenetically related to the norovirus. 9,29-32 Rotavirus infection can also cause an acute gastroenteritis mostly in children. Rotavirus infections are likely the most common cause of viral gastroenteritis in children, contributing to an approximately three million cases annually in the US, and sadly are linked to approximately 100 fatalities in the under 3 y.o. population, where some 90% show immunologic evidence of exposure. Natural immunity occurs following infection and is believed to protect individuals from repeat infections following an initial episode. Typical symptoms include vomiting, diarrhea, and dehydration that persist for a week or more, and necessitate prompt attention to rehydration early in the course of illness. In contrast to norovirus where an infective dose may be as few as 10 viral particles, rotavirus infection typically requires a larger infective dose, and occurs following an infective exposure of up to 100 viral particles. In both viral infections, the duration of incubation is 2 to 3 days in otherwise healthy individuals. 9

CASE STUDY: DINING OUT ON A CRUISE SHIP

Ms. J T was A 62 Y.O. retired female who presented at the Ship infirmary on the second day of her voyage. Upon arrival at the infirmary, she presented with complaints of severe abdominal cramps, watery diarrhea, and nausea, with an onset of early symptoms of nausea approximately 18 hours after embarking on the cruise, which she was unable to control by rest and fluids, and which became emergent within 24 hours of travel. Upon further investigation, she reported attending a buffet dinner hosted by the Ship's Captain the evening before, during which she reported consuming portions of various seafood items, including what appear to be uncooked shrimp and oysters. Ms. J.T.'s vital signs were generally normal with the exception of a mild fever typically not exceeding 102°F, abdominal tenderness upon palpitation, lethargy, mild dehydration, and non-life-threatening hypotension. Ms. J.T was followed by 11 additional passengers on the same day who presented with similar symptoms and chief complaints of mild fever, lethargy, watery diarrhea mile hypotension and abdominal tenderness upon palpitation, and who had attended and consumed the same buffet dinner, including the seafood entrees. The timing and cluster of patients was suggestive of an on-board food or water borne illness, and stool specimens were collected from the entire patient cluster for laboratory analysis in the infirmary laboratory. Initial on-board RIA rapid tests for norovirus were positive for all 12 patients, including Ms. J T. The medical team administered supportive therapeutic measures including 1) administering intravenous fluids to restore hydration; 2) immediate administration of Compazine (10 to 20 mg., I.M.); Sachets of 20.5 mg of WHO low osmolar formulae oral rehydration solutions (low osmolar Oral Rehydration Solution consisting of 2.6 g/L NaCl, 2.9 g/L Na-disodium citrate dihydrate, 1.5 g/L KCl, and 13.5 g/L anhydrous glucose) as needed to restore hydration. 31 3) In addition. Patients were administered two 20 mg tablets of loperamide initially and an additional tablet after each subsequent watery bowel movement thereafter until symptoms subsided; and 4, an 8 mg tablet of ondansetron was administered every 8 hours for symptoms of nausea until gastrointestinal symptoms subsided. Patients were released to their quarters within 4 hours to continue their oral

treatment regimen and returned to the infirmary periodically (~ 8 hours) to continue to monitor vital signs for up to 3 days thereafter. All patients continued the voyage and experienced a full recovery by the final port of call.

As a result of the outbreak, the on-board medical team implemented strict infection control measures, including isolation of affected passengers in the infirmary or their quarters, enhanced cleaning protocols in the food preparation and dining areas, care to dispose of uneaten leftovers, and promoted hand hygiene measures for all food service personnel, with recommendations for ship wide attention to periodic hand washing especially before dining. In a Public Health Response, the ship' s medical staff promptly reported the outbreak to relevant health authorities at the next port of call. Passengers were advised on proper hygiene practices, and the ship implemented additional sanitation measures to contain the spread of the virus.

The Outcome of the on-board incident was chalked up to experience. Over the following days, the number of reported cases decreased progressively as the implemented measures took effect. Mrs. J.T. and other affected passengers showed gradual improvement with supportive care. The cruise line faced scrutiny and implemented changes to food handling practices to prevent future outbreaks of norovirus or other common food borne agents that could negatively impact ocean going voyages.

In our experience, ORS treatment may lower the mortality rate of diarrhea by as much as 93%. Case studies in four developing countries also have demonstrated an association between increased use of ORS and reduction in mortality. ORT using the original ORS formula has no effect on the duration of the diarrheic episode or the volume of fluid loss, [12] although reduced osmolarity solutions have been shown to reduce both the magnitude of vomiting and stool volume.

In conclusion, this clinical case and the accompanying overview of agents linked to food and water borne illnesses underscores the challenges of managing infectious outbreaks on not only cruise ships but also exercising diligence during casual dining out at your favorite restaurant. Swift identification, isolation, and public health interventions are crucial in preventing further spread of FWBI and ensuring the well-being of passengers, crew members and casual diners especially while enjoying travel abroad.

REFERENCES

1. Centers for Disease Control and Prevention. Estimates of foodborne illness in the United States. CDC. Reviewed: November 5, 2018. https://www.cdc.gov/foodborneburden/estimates-overview.html.

2. Centers for Disease Control and Prevention. National Outbreak Reporting System (NORS). CDC. Updated: February 3, 2022. Available at: https://wwwn.cdc.gov/norsdashboard/.

3. Centers for Disease Control and Prevention. Parasites - Cysticercosis. CDC. Reviewed: September 22, 2020. Available at: https://www.cdc.gov/parasites/cysticercosis/index.html.

4. Centers for Disease Control and Prevention. Bacillus cereus food poisoning associated with fried rice at two child day care centers--Virginia, 1993. MMWR Morb Mortal Wkly Rep. 1994 Mar 18;43(10):177-8. PMID: 8121375

5. Centers for Disease Control and Prevention. Pathogens Causing US Foodborne Illnesses, Hospitalizations, and Deaths, 2000-2008. January 2012. https://www.cdc.gov/foodborneburden/pdfs/pathogens-complete-list-01-12.pdf.

6. Centers for Disease Control and Prevention. Listeria outbreaks. February 15, 2023. Available at: https://www.cdc.gov/listeria/outbreaks/index.html.

7. Centers for Disease Control and Prevention. Multistate outbreak of listeriosis associated with Jensen Farms cantaloupe--United States, August-September 2011. MMWR Morb Mortal Wkly Rep. 2011 Oct 7;60(39):1357-8. PMID: 21976119.

8. Weber AC, Levison AL, Srivastava SK, Lowder CY. A case of Listeria monocytogenes endophthalmitis with recurrent inflammation and novel management. J Ophthalmic Inflamm Infect. 2015 Dec;5(1):28. PMID: 26437938.

9. Tortola, G J. Funke, B.R. and Case, C.L. (Eds) Ch 25 In: Textbook of Microbiology, an Introduction. 11 th Ed.; Pearson Pubs, NY. IBSN 10-0-321-79310.2; IBSN 13-978-0-321-79310-2.

10. Flanagan PA. Giardia--diagnosis, clinical course and epidemiology. A review. Epidemiol Infect. 1992 Aug;109(1):1-22. PMID: 1499664.

11. Stanley SL Jr. Amoebiasis. Lancet. 2003 Mar 22;361(9362):1025-34. PMID: 12660071

12. Centers for Disease Control and Prevention. Parasites - Cysticercosis. CDC. 2020. Available at: https://www.cdc.gov/parasites/cysticercosis/index.html.

13. Brailita DM, Lingvay I, Aung K, Ojha AK. Amebic liver/hepatic abscesses. Medscape Drugs & Diseases from WebMD. Updated October 15, 2019. https://emedicine.medscape.com/article/183920-overview.

14. Yamamoto K, Yanagawa Y, Oka S, Watanabe K. Two cases of endoscopically diagnosed amebic colitis treated with paromomycin monotherapy. PLoS Negl Trop Dis. 2020 Mar 19;14(3):e0008013. PMID: 32191702.

15. Centers for Disease Control and Prevention. Bacillus cereus food poisoning associated with fried rice at two child day care centers--Virginia, 1993. MMWR Morb Mortal Wkly Rep. 1994 Mar 18;43(10):177-8. PMID: 8121375

16. Sanon, V., Sainvil, F., Tulp, O.L., Awan, A.A., Einstein, G.P. Haiti' s Cholera Epidemic: When the Unexpected Must be Expected. FASEB J. 35: S1, 2021.https://doi.org/10.1096/fasebj.2021.35.S1.03349

17. Severe, K., Alcenat, N., and Rouzier, V. Resurgence of Cholera in Haiti amidst Humanitarian Crises. N Engl J Med 2022; 387:2389-2391. DOI: 10.1056/NEJMc2213782

18. Taylor SL, Stratton JE, Nordlee JA. Histamine poisoning (scombroid fish poisoning): an allergy- like intoxication. J. Toxicol Clin Toxicol. 1989;27(4-5):225-40. PMID: 2689658

19. Lehane L, Lewis RJ. Ciguatera: recent advances but the risk remains. Int J Food Microbiol. 2000 Nov 1;61(2-3):91-125. PMID: 11078162

20. Magnussen A, Parsi MA. Aflatoxins, hepatocellular carcinoma, and public health. World J Gastroenterol. 2013 Mar 14;19(10):1508-12.

21. Zhang W, He H, Zang M, Wu Q, Zhao H, Lu LL, Ma P, Zheng H, Wang N, Zhang Y, He S, Chen X, Wu Z, Wang X, Cai J, Liu Z, Sun Z, Zeng YX, Qu C, Jiao Y. Genetic Features of Aflatoxin- Associated Hepatocellular Carcinoma. Gastroenterology. 2017 Jul;153(1):249-262.e2.

22. Stoll, A. (October 1932). "Ergot and ergotism". The Science of Nature. 20 (41): 752–757. Bibcode:1932NW..20.752S. doi:10.1007/BF01493390. S2CID 29050640.

23. Bianco MI, Luquez C, de Jong LI, Fernandez RA. Presence of Clostridium botulinum spores in Matricaria chamomilla (chamomile) and its relationship with infant botulism. Int J Food Microbiol. 2008 Feb 10;121(3):357-60. PMID: 18068252

24. Chamomile. Drugs and Lactation Database (LactMed) [Internet]. Bethesda, MD: U.S. National Library of Medicine. 2021. PMID: 30000867

25. Schardl, Christopher L.; Panaccione, Daniel G.; Tudzynski, Paul (2006). Ergot Alkaloids – Biology and Molecular Biology. The Alkaloids: Chemistry and Biology. Vol. 63. pp. 45–86. doi:10.1016/S1099-4831(06)63002-2. ISBN 978-0-12-469563-4. PMID 17133714.

26. Nichols D (May 24, 2003). Hypothesis on Albert Hofmann: Famous 1943 "Bicycle Day"". Hofmann Foundation.

27. Tulp OL, Mensah CP, Kakwere RT. Efficacy of Botulinum Toxin Stereotype A and Its Relevant Mechanisms of Action in Both Cosmetic and Therapeutic Uses. Curr Trends Toxi Pharma Res. 2021;1(1):1–6. DOI: 10.53902/CTTPR.2021.01.000503

28. World Health Organization (February 2017). "Tetanus vaccines: WHO position paper – February 2017" (PDF). Weekly Epidemiological Record. 92 (6): 53–76. hdl:10665/254583. PMID 28185446.

29. Widdowson MA, Sulka A, Bulens SN, et al. Norovirus and foodborne disease, United States, 1991-2000. Emerg Infect Dis. 2005 Jan;11(1):95-102. PMID: 15705329.

30. Bernstein DI (2009). Rotavirus overview. The Pediatric Infectious Disease Journal. 28 (Suppl 3): S50–S53. doi: 10.1097/INF.0b013e3181967bee. PMID 19252423. S2CID 30544613.

31. Lehane L, Lewis RJ. Ciguatera: recent advances but the risk remains. Int J Food Microbiol. 2000 Nov 1;61(2-3):91 125. PMID: 11078162

32. Virus Taxonomy: 2021 Release. International Committee on Taxonomy of Viruses (ICTV).

33. WHO. Oral Rehydration Salts (ORS). 1 January 2006.

34. Finkelstein, RA. Cholera, Vibrio cholerae O1 and O139, and Other Pathogenic Vibrios. Ch 24, In: Medical Microbiology. 4 th edition. UTMB Galveston. 1996.